DESIGN OF A COST-EFFECTIVE HYBRID RENEWABLE ENERGY SYSTEM IN A REMOTE AREA OF SOMALIA

By

Abdiaziz Ali Nur
21171003

A Project submitted to the Department of Electrical and Electronic Engineering in partial fulfilment of the requirements for the degree of
Master of Engineering in Electrical and Electronic Engineering

Department Electrical and Electronic Engineering
BRAC University
23 June 2022

Declaration

It is hereby declared that

1. The thesis submitted is my own original work while completing degree at BRAC University.
2. The thesis does not contain material previously published or written by a third party, except where this is appropriately cited through full and accurate referencing.
3. The thesis does not contain material which has been accepted, or submitted, for any other degree or diploma at a university or other institution.
4. I have acknowledged all main sources of help.

Student's Full Name & Signature:

_____

Abdiaziz Ali Nur
21171003

Approval

Project Titled **"Design of a cost-effective hybrid renewable energy system in a remote area of Somalia."** submitted by

Abdiaziz Ali Nur (21171003)

of Spring, 2022 has been accepted as satisfactory in partial fulfilment of the requirement for the degree of Master of Engineering in Electrical and Electronic Engineering on 23 June 2022.

Examining Committee:

Supervisor:
(Member)

_____
A. S. Nazmul Huda, PhD
Assistant Professor, Dept. EEE
BRAC University

Internal Examiner:
(Member)

_____
Abu Hamed M. Abdur Rahim, PhD
Professor, Dept. EEE
BRAC University

Departmental Head:
(Chair)

_____
Md. Mosaddequr Rahman, PhD
Professor and Chairperson, Dept. EEE
BRAC University

Abstract

Due to the availability of distributed generators (DG). The structure, complexity, and design of power systems are changing in the modern day. Climate change is an additional concern, as limiting global warming to 1.5°c will require a rapid and sustained reduction in Green House Gas (GHG) emissions, including a 45% reduction in global carbon dioxide emissions by 2030. Renewable energy is clean, eco-friendly, and reliable. This thesis examines the Design of cost effective hybrid renewable energy system in a remote area of Somalia. Renewable energy resources are located in Dusmareb, Somalia. The LCOE is 0.153$/kWh, compared to 0.6$/kWh on the grid in a given region. The system is capable of supplying the load demand. HOMER Pro is used to perform optimization and sensitivity analysis. The system is designed and simulated using Matlab/Simulink. The Perturb and Observe MPPT algorithm is utilized to extract the highest amount of energy possible from the photovoltaic and wind systems.

Keywords:

Cost-Effective, Hybrid, Microgrid, Design, Somalia Standalone, Remote area, Dusmareb.

Dedication

This work is completely dedicated to my respectful **parents, brothers and sisters**, without the whose constant support, this thesis paper was not possible. They always inspire me.

Acknowledgement

It gives me great pleasure to appreciate all those who have encouraged and helped me heartedly in bringing my project to completion. To begin, I would want to express my gratitude to ALLAH almighty for the grace-filled blessings and for bringing this to a successful conclusion.

I would like to convey my heartfelt appreciation to my supervisor, **Dr. A. S. Nazmul Huda**, for his guidance throughout the project's discussions. I value this opportunity to collaborate with such a supervisor on successfully completing this project as one of the most valuable in my career.

Finally, I would like to show my thankfulness to **Prof. Shahidul Islam Khan**, the department's graduate coordinator, and all department faculty members for their assistance.

Contents

Declaration ..... **I**

Approval ..... **II**

Abstract ..... **III**

Dedication ..... **IV**

Acknowledgement ..... **V**

Contents ..... **VI**

List of Tables ..... **IX**

List of Figures ..... **X**

CHAPTER 1 ..... **1**

Introduction **1**

1.1 Background 1

1.2 Statement of The Problem 1

1.3 Motivation 2

1.4 Project Objectives 2

1.5 Project Scope 3

1.6 Thesis Structure 3

CHAPTER 2 ..... **4**

Literature Review **4**

2.1 Distributed Generation and Microgrid Development 4

2.2 Microgrid Operation 5

2.3 Microgrid Energy Management and Control 5

2.4 Renewable Energy Sources and Storage Battery 6

2.4.1 Solar Photovoltaic 6

2.4.1.1 Solar Cell 6

2.4.1.2 Types of Solar Modules and Their Arrangement 7

2.4.2 Wind Energy 9

2.4.2.1 Wind Energy Extraction 9
2.4.2.2 Classification and Components of Wind Turbine 11
2.4.3 Battery Storage 12
2.5 Related Work 13
CHAPTER 3 15
Methodology 15
3.1 Introduction 15
3.2 Data Analysis Techniques 17
3.3 Economic Analysis 17
3.3.1 Renewable Energy Resources of Selected Site 17
3.3.1.1 Solar Energy Resource 17
3.3.1.2 Wind Energy Resource 19
3.3.2 Energy Demand and Load Profile 19
3.3.3 Sizing of Standalone Hybrid Systems 21
3.3.3.1 PV Modules and PV Area Calculation 21
3.3.3.2 Sizing of Wind Turbine 23
3.3.3.3 Battery Sizing 23
3.3.3.4 Charge Controller Sizing 24
3.3.3.5 Inverter Sizing 25
3.3.4 System Cost 25
3.3.4.1 Capital Investment Costs 26
3.3.4.2 Costs of Operation and Maintenance (O&M) 26
3.3.4.3 Cost of Replacement: 26
3.4 System Modelling 27
3.4.1 Photovoltaic Model 27
3.4.2 Boost Converter Modelling 29
3.4.3 Wind Turbine 31

3.4.4 Bidirectional Converter and Storage Battery.....33
3.4.5 Inverter.....34
3.4.6 Model of a Hybrid Microgrid System in MATLAB/SIMULINK.....35
CHAPTER 4.....36
Simulation Result and Analysis.....36
4.1 Introduction.....36
4.2 HOMER Pro Model.....36
4.2.1 Result from HOMER Pro Simulation.....36
4.3 Matlab/Simulink Result.....39
CHAPTER 5.....45
Conclusion.....45
5.1 Future Work.....45
5.2 Limitations.....45
Reference.....46
Appendix.....49
A.1. Matlab Code for Parameter Calculation.....49
A.2. System Cost Summary from HOMER Pro.....50
A.3. Drive Drain and Pitch Control Model of Wind Turbine.....50

List of Tables

Table. 3 1. Single house daily load consumption 20
Table. 3 2. Electrical characteristics of selected module 21
Table. 3 3. Characteristics of wind turbine model used in matlab/Simulink 23
Table. 3 4. Battery parameters 23
Table. 3 5. Initial capital cost of hybrid system main components 26

List of Figures

Fig. 2. 1. Types of distribution generators 4
Fig. 2. 2. Microgrid operation a) Grid-connected mode b) Standalone mode 5
Fig. 2. 3. Energy band diagram in semiconductors 7
Fig. 2. 4. Different types of PV modules and their configurations 7
Fig. 2. 5. The equivalent circuit of solar cell 8
Fig. 2. 6. I-V characteristics of solar cell 8
Fig. 2. 7. Airfoil 9
Fig. 2. 8. Mas of column ρAV 10
Fig. 2. 9. Wind turbine real view 12
Fig. 3. 1. Architecture of a hybrid standalone microgrid system 15
Fig. 3. 2. Flow chart of the project work 16
Fig. 3. 3. Dusmareb city, central Somalia (google map view) 18
Fig. 3. 4. Dusmareb monthly solar radiation 18
Fig. 3. 5. Monthly average temperature 19
Fig. 3. 6. Monthly wind speed 19
Fig. 3. 7. Daily average load demand 20
Fig. 3. 8. Simulink model of solar PV array 28
Fig. 3. 9. I-V and P-V characteristics of photovoltaic array by varying solar irradiation 28
Fig. 3. 10. The effect of temperature on P-V characteristics of PV array 29
Fig. 3. 11. Simulink model of boost converter with MPPT 29
Fig. 3. 12. P & O method code 30
Fig. 3. 13. Block diagram of WECS 31
Fig. 3. 14. Power characteristics of a wind turbine 32
Fig. 3. 15. The Simulink model of a wind turbine system 33
Fig. 3. 16. Bidirectional and battery Simulink model 34
Fig. 3. 17. Simulink model of an inverter 35
Fig. 3. 18. Overall System Modelling in Simulink 35
Fig. 4. 1. HOMER diagram for the system architecture 36
Fig. 4. 2. Monthly electricity production 37
Fig. 4. 3. Total electricity generation with excess power 37
Fig. 4. 4. Load demand and power generation 38
Fig. 4. 5. Load power system power 38

Fig. 4. 6. NPV of the system components....39
Fig. 4. 7. Variation of an irradiation with time....39
Fig. 4. 8. PV-power output at MPPT....40
Fig. 4. 9. Output voltage of PV....40
Fig. 4. 10. Wind turbine AC output voltage....41
Fig. 4. 11. Wind turbine output current....41
Fig. 4. 12.Wind turbine output power....41
Fig. 4. 13. Battery output Voltage....42
Fig. 4. 14. Battery output current....42
Fig. 4. 15. State of charge and discharge of the battery....43
Fig. 4. 16. DC bus output voltage....43
Fig. 4. 17. Load voltage and current....44
Fig. 4. 18. Load power (kW)....44

CHAPTER 1

Introduction

1.1 Background

Electricity has become crucial to modern society due to its use in various applications such as lighting, heating, communication, and powering common electronics, all of which have impacted how we live and do things [1].

Climate change is a significant topic in today's globe. According to the COP 26 summit, limiting global warming to 1.5 degrees Celsius will require a rapid and persistent reduction in Green House Gas (GHG) emissions, including a 45 percent reduction in global carbon dioxide emissions by 2030 [2]. As a result, numerous enterprises worldwide began shifting their electricity production away from conventional energy sources and toward renewable energy sources. Apart from industries, many countries have electrification targets for rural and sub-urban areas.

The expansion of existing networks intensifies the difficulties faced by power engineers. As a result, renewable energy sources are becoming more viable as a source of electricity in rural and suburban regions. The growing energy demand, the depletion of fossil fuels, and the attendant environmental damage have shifted global attention to renewable energy sources. In terms of cost, efficiency, and reliability, hybrid integration of two or more renewable energy sources is more effective than a single source. Solar and wind energy have become competitive with conventional energy sources due to lower manufacturing costs and improved efficiency.

1.2 Statement of The Problem

Numerous communities in underdeveloped countries that lack access to electricity can benefit from these distributed generators. Somalia is one of these countries that lacks an adequate energy supply [3]. The country faces three key electrification challenges in rural and sub-urban areas: a lack of access to electricity, an exceptionally high cost per unit, and low reliability. There is a lack of reliable statistical data on the energy situation in Somalia, as the country has only undertaken a few studies in recent years. According to the World Bank, 36.033 percent of Somalia's population has electricity in 2019, relative to 11.12 percent in rural areas [4]. However, demand has increased, and new small industries have emerged. On the other hand, rural electrification is critical in of entire country. Thus, the microgrid based on renewable energy can contribute to the electrification of the country.

This work aims to analyze, optimize and design the standalone hybrid renewable energy system in Dusmareb, Somalia. Powerful techniques were used, such as a maximum power point tracking system to extract the maximum power from solar PV and wind turbine systems. The result is analysed by using Matlab/Simulink.

Moreover, the economic feasibility of the hybrid PV/Wind/Battery system was studied using HOMER Pro software by utilizing the potential of solar and wind energy in the selected location to analyze the Levelized Cost of Electricity (LCOE).

1.3 Motivation

Somalia has the highest potential for renewable energy resources among any other African country. The country has sufficient sunlight and wind to meet the basic electricity requirements. Small wind turbines and solar panels can provide enough energy to charge batteries and light lamps. These could be the first steps in removing the shortage of electricity access in developing countries like Somalia where basic energy is scarce.

Previously, the cost of solar panels and small wind turbines discouraged investment in developing countries. Renewable energy sources (RES) such as photovoltaic solar panels, wind turbines, and batteries have evolved in technology, making renewable energy investments possible.

One possible answer to these issues is a hybrid renewable energy systems. People in Dusmareb and many other Somali cities require clean, hygienic water, lighting to read books and learn in a clean, non-polluted environment, and food cooked without charcoal wood. A standalone hybrid microgrid with cost effective has been built to increase the city's living standard, reduce electricity costs, and contribute to global warming reduction.

There are two reasons for the increased price per unit of power in Dusmareb and other regions of Somalia. Fuel imports from other countries and unreliable diesel generators. This work tries to eliminate that two problems by utilizing the renewable energy sources.

1.4 Project Objectives

The main two objectives of this project are:

- To utilize free renewable energy available in sub-urban areas of Somalia without causing any harmful effects to the environment and human lives.
- To study the economic feasibility of the standalone hybrid renewable energy in sub-urban locations in Somalia.

There are other engineering objectives of this project, including,

- To design a hybrid wind/PV/Battery standalone system in MATLAB/SIMULINK.
- To control the system voltage and power.
- To design a bi-directional charge controller with MPPT to protect the battery bank.
- To design the hybrid wind/PV/Battery system in HOMER Pro software to analyze the sensitivity and Levelized Cost of Electricity (LCOE).

1.5 Project Scope

The purpose of this project is to determine the cost-effective hybrid system based on renewable energy for electrification in a rural and sub-urban city in Somalia, more specifically in the case study of Dusmareb. Additionally, the study designed a hybrid photovoltaic/wind/battery autonomous renewable energy system in Matlab/Simulink using renewable energy sources available in the selected location.

1.6 Thesis Structure

The thesis is structured as follows.

Chapter one discusses the background of the work, the challenges that will be attempted to answer, and what prompted the writer to conduct the research.

Chapter two discusses the existing literature review for this work, including journals, conference papers, articles, and background knowledge.

The third chapter discusses the research background, methodology, data analysis approach, and overall thesis design, which includes system sizing and economic considerations.

Chapter four summarizes the simulation results from HOMER Pro and Matlab/Simulink.

Finally, Chapter 5 summarizes the thesis, makes recommendations, and discusses the work's limitations.

CHAPTER 2

Literature Review

2.1 Distributed Generation and Microgrid Development

The Distributed Generation (DG), also known as On-Site Generation (OSG), refers to the generation and storage of electricity using a range of distributed energy resource (DER) technologies located close to the customer's loads [5]. As seen in Fig. 2.1, these technologies are referred to as distributed generators [6]. Hybrid Microgrids comprise various distributed generators such as solar panels, small wind turbines, fuel cells, energy storage systems, and occasionally backup generators. Due to its proximity to end customers, the hybrid microgrid is a low- and medium-voltage system. It comprises a variety of energy-producing sources, most notably renewable energy sources, controllable energy management systems, and energy storage devices or batteries.

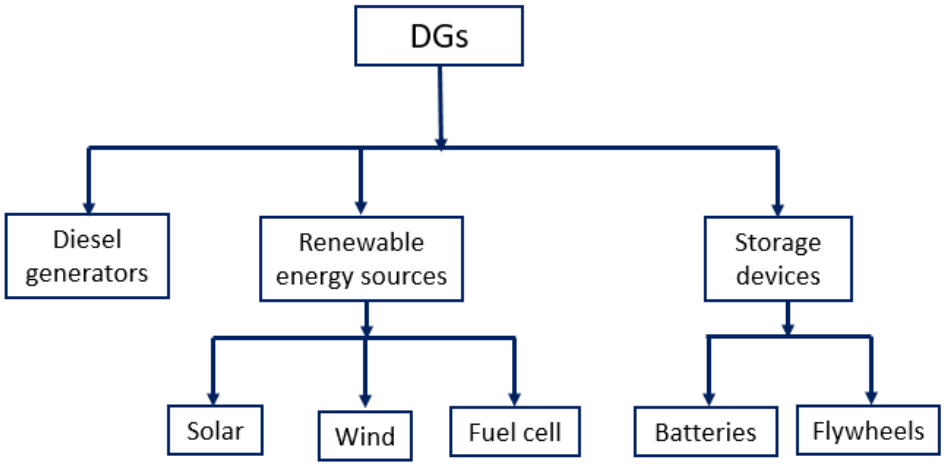

Fig. 2. 1. Types of distribution generators

While the majority of previous research on microgrids has concentrated on the integration of solar photovoltaic (PV), energy storage, and backup power generators, the current work expands on the investigation of integrating small wind turbines in windy areas to ensure the system's stability and long-term operation. Microgrid studies are divided into the feasibility and economic studies and control and optimization studies. A microgrid's structure can be either AC or DC. With many power electronic converters, it can be the future energy system in terms of reliability and power supply efficiency. These power electronic devices enable the microgrid to provide its maximum power as a controllable unit to meet customers' demands.

2.2 Microgrid Operation

The following modes of operation are recognized and defined for microgrids [7]. Grid-connected mode, alternatively referred to as on-grid mode, and off-grid mode, alternatively referred to as a standalone microgrid. The grid-connected mode, seen in Fig. 2.2 a, connects the microgrid to the national grid network. The microgrid can draw power from or supply it to the electrical grid. A point of common coupling is the term used to describe the point of connection to the utility grid. The structure of the isolated microgrid is depicted in Fig. 2.2 b. It is completely disconnected from the utility grid. The microgrid power system should be capable of supplying the intended load without the assistance of any other source of electricity. It is well suited for islanded regions and distant areas where access to the utility grid is difficult. The focus of this project is on the standalone microgrid.

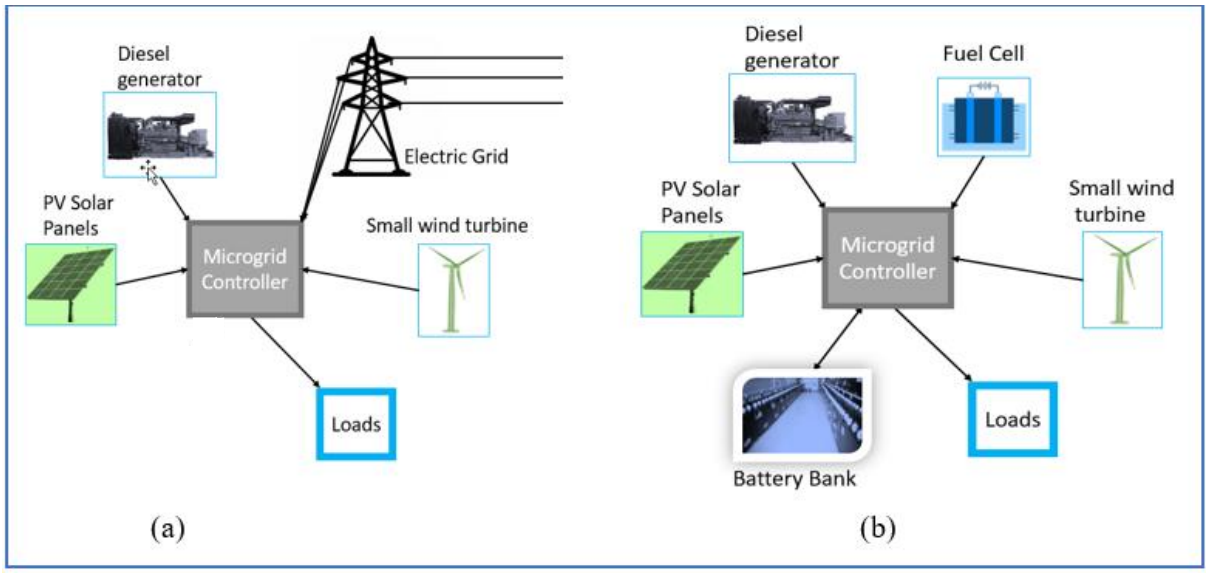

Fig. 2. 2. Microgrid operation a) Grid-connected mode b) Standalone mode

2.3 Microgrid Energy Management and Control

A control system is essential to ensure that operations remain steady at all times [8]. It operates in an islanded mode to maintain voltage and frequency levels. Thus, microgrid control is critical for the self-sustainability of future grids. General Microgrid management is a sophisticated multi-objective control system that addresses issues spanning several technology domains, temporal spans, and physical dimensions [9]. Thus, the energy management system for the microgrid is divided into three control stages.

1) Primary Control Stage: Primary controls are the lowest level of the control hierarchy and have the quickest response. Off-grid detection, equalization control, converter output control, and voltage/frequency regulation are the primary control operations.

2) Secondary Control Stage: The secondary stage is responsible for the microgrid system's reliability and economic operation. Secondary control functions include power management and generation control. By optimizing power generation and management, system costs can be reduced and efficiency increased. Additionally, secondary control modulates the energy flow based on the battery's state of charge.

3) Tertiary Control Stage: This is the microgrid system's final control stage. It is responsible for controlling and maintaining the system's intelligence. Tertiary control of the microgrid system takes the energy balance between consumed and generated energy into account.

2.4 Renewable Energy Sources and Storage Battery

Today, the demand for electrical energy is growing at a breakneck pace. The depletion of conventional energy sources and significant influence on the environment, particularly greenhouse gas emissions, contribute to ecological imbalance [10]. Thus, an alternate energy source is non-conventional energy sources, which significantly satisfy the world's energy demands. These renewable energy sources are clean, eco-friendly, and reliable. This section discusses the renewable energy source and energy storage system used in this project. We will discuss the evolution of photovoltaic solar technology, wind turbine technology, and battery technology. All three components' mathematical basis and operation will be discussed.

2.4.1 Solar Photovoltaic

The photovoltaic effect is the process of directly converting sunlight into electricity. The sun's energy is truly enormous: the earth's surface receives roughly 1.2×10^{17} W of solar power on average. The sun is the principal source of most other renewable energy sources. Photovoltaic power generation is reliable, has no moving components, and has low operating and maintenance costs. A photovoltaic system is completely silent and does not pollute the environment. Photovoltaic systems are modular and straightforward to set up. Without the need for transmission lines, power can be generated where it is needed. Solar electricity is already less expensive than other small power sources, such as diesel generators. Light-to-electricity conversion, or photovoltaic, is now recognized as an essential power generation method. Manufacturing output has increased at around 20% yearly for the last decade and may reach gigawatts in the next decade [11].

2.4.1.1 Solar Cell

In a photovoltaic system, the solar cell is the smallest unit of energy conversion. They are constructed of semiconductors [12]. Solar cells are typically integrated into modules for

practical operation. The modules have a 20-year life expectancy and their best production efficiency is close to 18% [13]. The operation of a solar cell is dependent on semiconductors' capacity to convert sunlight to energy via the photovoltaic effect. Quantum theory dictates that the energy of an electron within a crystal must lie within well-defined bands. The energies of valence orbitals with form bonds between atoms define precisely this band of states, the valence band. The conduction band is the next higher band, separated from the valance band by an energy gap, or bandgap. The bandgap width $E_c - E_v$ is a critical property of semiconductors and is typically indicated by E_g. The band diagram and electron-hole distribution in a semiconductor are depicted in Fig. 2.3.

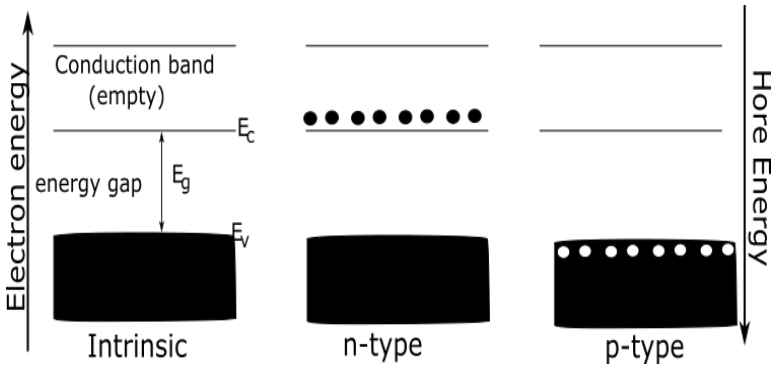

Fig. 2. 3. Energy band diagram in semiconductors

2.4.1.2 Types of Solar Modules and Their Arrangement

Numerous solar cell types are already available on the market, and further types are being developed. Crystalline silicon dominates the market. These cells are increasingly constructed using multicrystalline material to keep costs down. Fig. 2.4 illustrates the types and configurations of the most widely used photovoltaic panels today [14], [15].

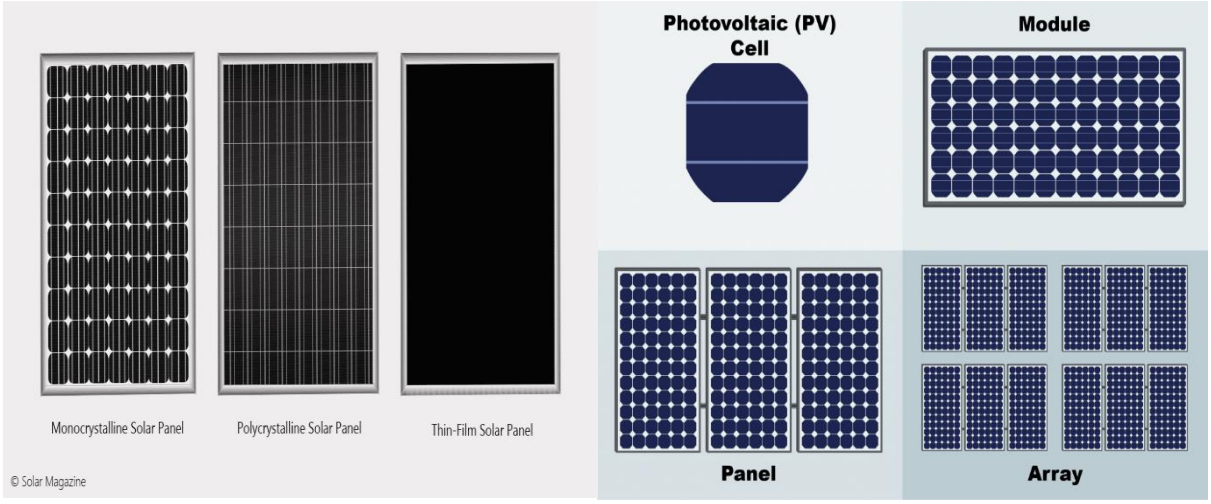

Fig. 2. 4. Different types of PV modules and their configurations

The I_V characteristics of a solar cell can be obtained by drawing an equivalent circuit of the device Fig. 2.5. The generation current I_L in parallel with diode with represents the p-n junction and resistance.

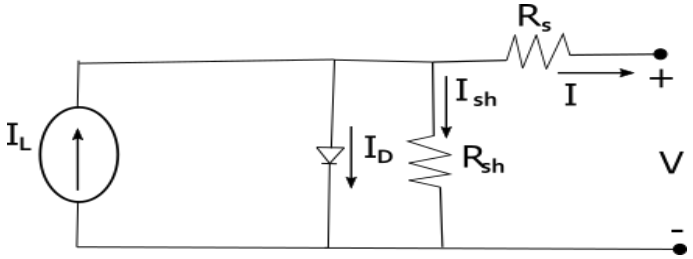

Fig. 2. 5. The equivalent circuit of solar cell

$$I_L = I_D + I_{sh} + I \tag{2.1}$$

$$I = I_L - I_D - I_{sh} \tag{2.2}$$

The diode current for the solar cell is given as

$$I_D = I_o \left[\exp\left(\frac{qV}{KT}\right) - 1\right] \tag{2.3}$$

The shunt current of the solar cell is given as

$$I_{sh} = \frac{V + IR_s}{R_{sh}} \tag{2.4}$$

The output current or short circuit current I can be shown Shockley equation by substituting the equation 2.3 and 2.4 into equation 2.2.

$$\mathrm{I} = I_L - I_o \left[\exp\left(\frac{qV}{KT}\right) - 1\right] \tag{2.5}$$

Where I is the current, V is the voltage, K is the Boltzmann constant, q is the magnitude of the electron charge, and T is the absolute temperature. The output circuit voltage of I_V characteristics when I = 0 can be obtained.

$$V_{oc} = \frac{KT}{q} \ln\left(\frac{I_L}{I_o} + 1\right) \tag{2.6}$$

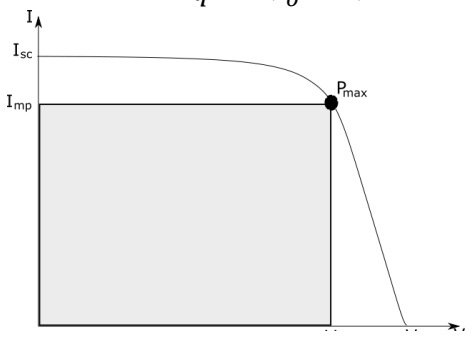

Fig. 2. 7. I-V characteristics of solar cell

No power is generated under a short circuit or open circuit since in a short circuit voltage is zero while in an open circuit current is zero. The maximum power P_{max} produced by the device is reached at a point on the characteristics where the product of $V_{mp}I_{mp}$ is maximum. Fig. 2.6 depicts the I-V characteristics of a solar cell. The position of the maximum power point usually defines the fill factor FF. The following equation related the fill factor, maximum operating voltage, current, and the maximum power of the solar cell.

$$P_{max} = V_{mp}I_{mp} = FFV_{oc}I_{sc} \tag{2.7}$$

Where the fill factor can be calculated by using equation 2.8.

$$FF = \frac{V_{mp}I_{mp}}{V_{oc}I_{sc}} \tag{2.8}$$

2.4.2 Wind Energy

The wind is the natural flow of air and it is what converts solar energy into electricity. Due to the uneven heating of the atmosphere, around 2% of the total solar flux that reaches the earth's surface is converted to wind energy. Worldwide cumulative installed wind energy capacity has increased rapidly from the beginning of the third millennium, reaching 733 GW by the end of 2020 [16].

2.4.2.1 Wind Energy Extraction

Wind energy is the kinetic energy of massive quantities of air moving across the surface of the earth. Through the use of airfoils, a drive train, and a generator, a wind energy conversion system (WECS) converts this kinetic energy into mechanical and electrical energy. Air flows over a blade called an airfoil, which is similar to an airplane wing or propeller. As illustrated in Fig. 2.7, airflow over a stationary airfoil generates two forces: a lift force perpendicular to the airflow and a drag force in the direction of the airflow. Drag force is utilized to propel the parachute, which tugs on a rope. Hence, drag force is used in mechanical applications, but lift force is more suited to electricity generation [16].

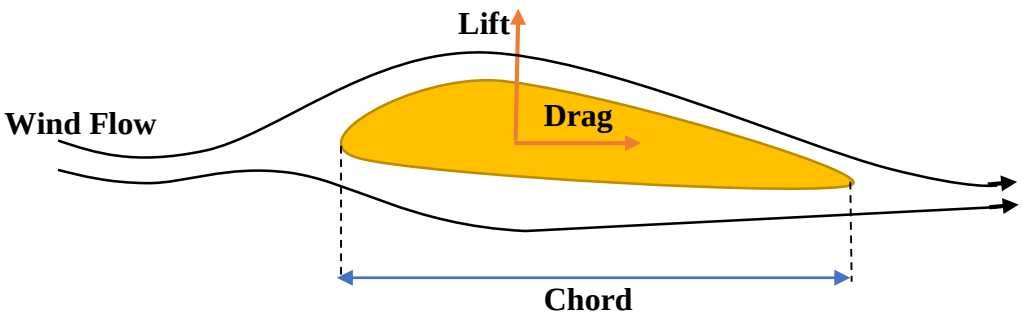

Fig. 2. 9. Airfoil

Wind kinetic energy can be considered, which is a function of the mass and velocity of the air volume. With a fixed air density (mass per unit volume), wind energy can be expressed as a function of speed.

$$E_c = \frac{1}{2}mV^2 \quad (2.9)$$

Where

m = mass of air volume (in kg)

V = instantaneous wind speed (in m/s)

E_c = kinetic energy (in joules

At normal atmospheric pressure and a temperature of 15°C (60°F), air weights approximately 1.225 kilograms per cubic meter (0.0763 lb/ft3). However, as humidity increases, the density decreases significantly. Similarly, cold air is denser than warm air, as the air density is lower at higher altitudes (in the mountains) due to the lower air pressure. As a result, the air's mass increases. $m = \rho V$ (2.10)

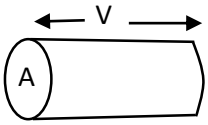

Fig. 2. 11. Mas of column

ρAV

In the unaltered situation depicted in Fig. 2.8, a column of wind upstream of the turbine intersects with the turbine disk's cross-sectional A. Equation 2.9 then becomes.

$$E_c = \frac{1}{2}(\rho AV)V^2 \quad (2.11)$$

Because density is a function of height and meteorological conditions, wind speed varies with height and location, but we are considering the general case here, which implies that speed and air density are constant over time and the area of the air column. When approaching turbine blades, the air slows down, and the power generated by the wind is proportional to the wind speed cubic (V^3). The amount of energy that can be taken from wind is calculated using equation 2.12.

$$P = \frac{1}{2}e \times k \times A \times \rho \times V^3 \quad (2.12)$$

Where

e = efficiency of the blades

k = conversion factor for unit (e.g. ft. lb to kw)

A = outer swept area of the blades (πr^2)

V = velocity of wind for enough upstream

ρ = density of air approximately 1.22 kg/m^3(0.0763 lb/ft^3) at sea level.

The theoretical maximum energy that can be extracted from wind is formulated by German Albert Betz in 1919, equation 2.13 shows the Betz Limit.

$$P_{max} = C_p \times P \tag{2.13}$$

C_p, the power coefficient is the ratio of power extracted by a wind turbine to power available in wind at that location, as Betz derived the value of C_p is 16/27 or 0.593 [17]. So in equation 2.13, the theoretical maximum of 59.3% of available power can be extracted. Practically a typical maximum of 30% including gearbox, generator, or pump losses is achieved. Wind turbines can produce energy at a minimum wind speed near 3.6 ms^{-1}, but requires a speed above 5 ms^{-1} to economically viable [18].

2.4.2.2 Classification and Components of Wind Turbine

There are two methods to drive generators. Direct drive generator, in this method the wind wheel directly turns the generator which was low speed unit 2) Transmission mounted, this method used gearbox which increases the rotor rpm by a factor called gear ratio typically 4, 5 or more. Wind Energy Conversion System (WECS) can be AC type WECS or DC type WECS [13]. An AC type uses Synchronous generators that can produce alternating current that can be fed directly to the load or grid. The DC type involves DC generators or other electronic mechanism that produce Direct Current that can be stored in the batteries or given to DC load, Wind turbine can be installed into offshore wind turbine site and offshore wind turbine site. The components of a wind turbine are shown in Fig. 2.9. The generator, gearbox, hydraulic system, and yawing mechanism are all housed in the Nacelle. The wind vane detects the direction of the wind and sends a signal to the controlling computer, which activates the yaw mechanism, causing the rotor to face the wind. The hub is the solid centre of the turbine, where the blades are attached. Wind turbines are classified as horizontal axis wind turbines or vertical axis wind turbines based on the orientation of their rotor's rotation axis. The rotor axis of horizontal axis turbines is kept horizontal and aligned parallel to the wind stream direction. The rotor in vertical axis turbines is vertical and fixed. It maintains a perpendicular relationship with the wind steam. Because wind is not a constant source of energy, it cannot meet all of the needs of consumers on its own. It must be integrated with other sources in order to provide a continuous backup. Wind Electric Generators (WECs) operate in one of the three modes 1) Standalone 2) Grid connected mode and 3) Backup mode [19].

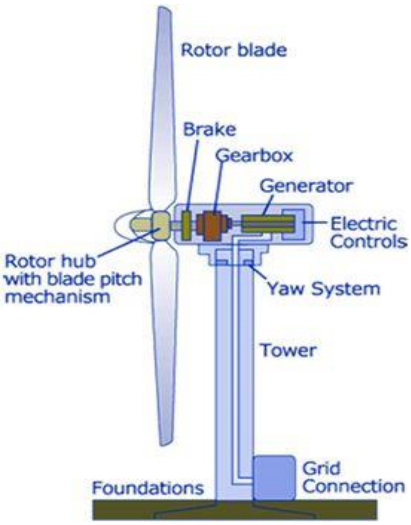

Fig. 2. 13. Wind turbine real view

2.4.3 Battery Storage

A standalone hybrid renewable energy system requires energy storage devices [20]. Batteries are electrochemical energy storage devices that allow for the chemical storage of energy and subsequent release when required. Batteries offer a higher energy density than alternative energy storage technologies such as super capacitors, fuel cells, compressed air systems, and flywheels. A storage system can help identify a mismatch between the electrical load and the renewable energy resource and facilitate overall system control and operation by smoothing out load fluctuations and adjusting for seasonal variations in renewable energy sources [21]. Several battery types are commonly employed in hybrid standalone microgrid systems. The two mainly used are Lead-acid batteries and lithium-ion batteries. [22]. Lead-acid batteries are applicable in hybrid isolated microgrids. It can exist at three voltage levels: 6 volts, 12 volts, and 24 volts. Lead-acid batteries are of two types flooded cells and sealed/gel cells. A flooded cell can be either flat or tubular. Electrodes are entirely submerged in an electrolyte. An immobilized electrolyte is present in lead-acid sealed/gel batteries. They require no upkeep at all. Lead-acid batteries last a long time and have a shallow discharge depth. Lithium-ion batteries are not used in hybrid standalone applications since they are more expensive than lead-acid batteries. Battery banks' State of Charge (SOC) should be limited to prevent them from harm and increase their usable life [23]. Several essential issues must be addressed when designing battery storage for a freestanding hybrid system [24]. 1) Rated battery capacity: This value shows the maximum energy that the battery can produce in a single discharge at the specified discharge rate and temperature.

2) Temperature compensation: The majority of batteries have temperature sensitivity. As a result, cold batteries cannot deliver the same level of power as hot ones.

3) Depth of discharge: In comparison to overall charge capacity, depth of discharge is the percentage of battery capacity (Ah) drawn from the battery.
(4) State of charge (SOC): The state of charge refers to the battery's remaining capacity at any particular time. It is one less than the Depth of Discharge (DOD) in percentage terms.
(5) Cycles of battery life: The life of any battery is difficult to predict because it is affected by several parameters such as depth of discharge, charge and discharge rate, operating temperature, and cycle count.
(6) Days of autonomy: The number of days the battery system can discharge energy continuously at a particular load without being replenished by the hybrid system.

2.5 Related Work

The Microgrid Energy Management System and Standalone Photovoltaic System Control case study is being conducted in Ethiopia's Ambo University Information Centre Technology Building [7]. This work is entirely focused on photovoltaic systems and batteries. Additionally, it considers the load's relatively small size, such as 30kwp. An islanded diesel-PV battery system was placed in Somalia to investigate a hybrid micro-grid in Garowe [25]. This paper focused on integrating a photovoltaic system with an existing diesel generator; therefore, the system is not emission-free, and the writer neglected to mention the system's economic feasibility.

First, the energy potentials of the Sub-Saharan region are described, as well as several problems that obstruct rural electrification efforts in this section of the continent. HOMER is used to model electrification solutions for the Rwamiko hamlet in Rwanda, and a microgrid consisting of PV, batteries, and a micro-hydro is evaluated. A feasibility study on how to supply energy to a sampling home load in Hargeisa was conducted. The paper only uses HOMER Pro software, implying that the author concentrated solely on the viability of the hybrid system. As a result, there is no system control in this study [26].

Article [27] provides instructions and technical techniques for designing a standalone solar home system, from site evaluation to component sizing. For first off, it only applies to small-scale PV systems and does not take into account any cost-related information.

Evaluation of Solar Home System Equipment in Bangladesh is determined by the technical quality of the SHS's component parts. During a technical audit of the SHS of IDCOL's (Infrastructure Development Company Limited) Rural Electrification and Renewable Energy Development Project, commonly used Solar Home System equipment was evaluated in the lab

(RREDP). Solar Home System components were gathered at random from IDCOL-approved vendors, manufacturer manufacturing lines, and the field. These items were evaluated in the laboratory. [28] examines the test findings before recommending a review for upgrading the technical standard based on field and laboratory experiences.

Wind resource evaluation in the Republic of Djibouti was measured using wind speed data from meteorological stations at eight locations over a three-year period. With mean annual wind speeds of more than 6.0 m/s, the results confirmed that three of the eight places (GaliMaaba, Ghoubbet, and Bada Wein) have the best resource. Wind simulations utilizing the NCEP-CFSR and ERA5 models demonstrate that seasonal fluctuations are stable across years and are broadly comparable with observed wind speed. The work simply assessed wind data and predicted the future wind energy resource in Djibouti [29].

The current work differs from all previous studies in that it combines all previous studies, including renewable energy assessment, whether solar or wind, and because previous studies in Somalia only performed feasibility studies based on HOMER, this study includes system design using Matlab/Simulink by controlling voltage and current.

In conclusion, the project focused on first collecting renewable energy data, then modeling the daily energy demand of 60 dwellings, then sizing and simulating the system using HOMER Pro and Matlab/Simulink, and finally analysing the result

CHAPTER 3

Methodology

3.1 Introduction

In the past few years, renewable energy sources have earned a large market in developing countries for their lack of sufficient energy, especially in Somalia, which is utilized in hospitals, commercial compounds, rural areas, and towns. The leading electricity supply providers in Somalia are already installed grid-connected solar PV systems of more than 100MWp. There are several semi-urban locations where transmission lines are not possible to reach. The diesel generators are employed in such places, unreliable and not cost-effective for those populations. This project explores the cost-effectiveness and design of a hybrid PV/wind/battery islanded system in Dusmareb city, central Somalia. Fig. 3.1 shows the architecture of proposed hybrid standalone renewable energy system.

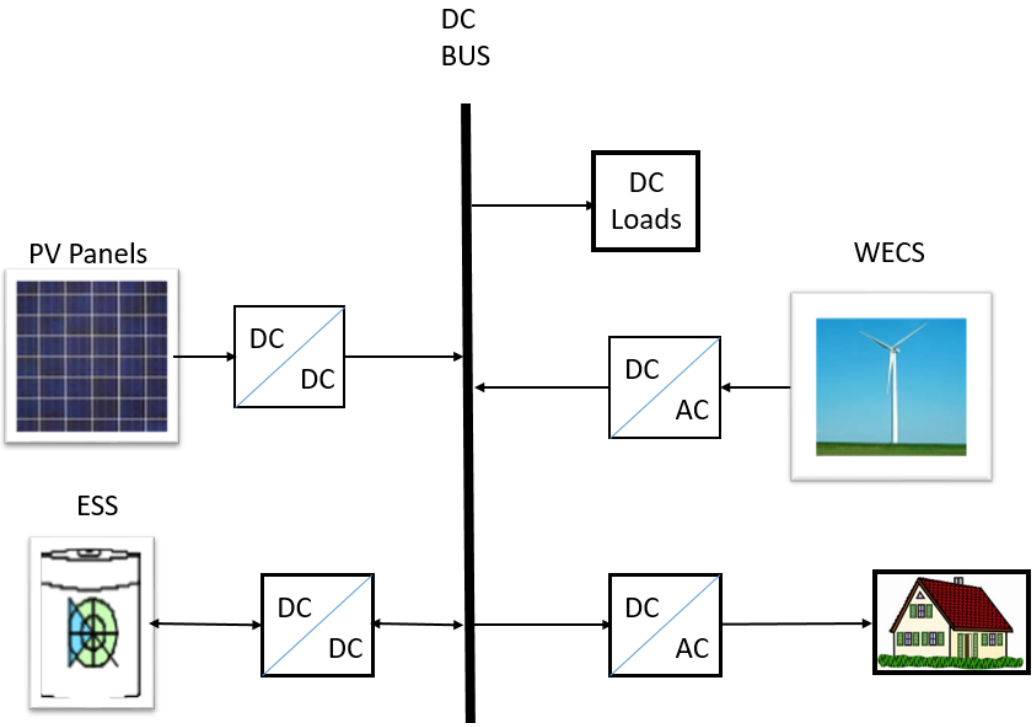

Fig. 3. 1. Architecture of a hybrid standalone microgrid system

Fig. 3.2 illustrates the flowchart of the prosed project. A specified site's solar and wind statistics are investigated based on data acquired from several sources such as global Atlas and NASA. The daily load curve of 60 residences was calculated by considering the electrical appliances

and their hours in use. The obtained data and load profile is then applied to design the standalone hybrid system.

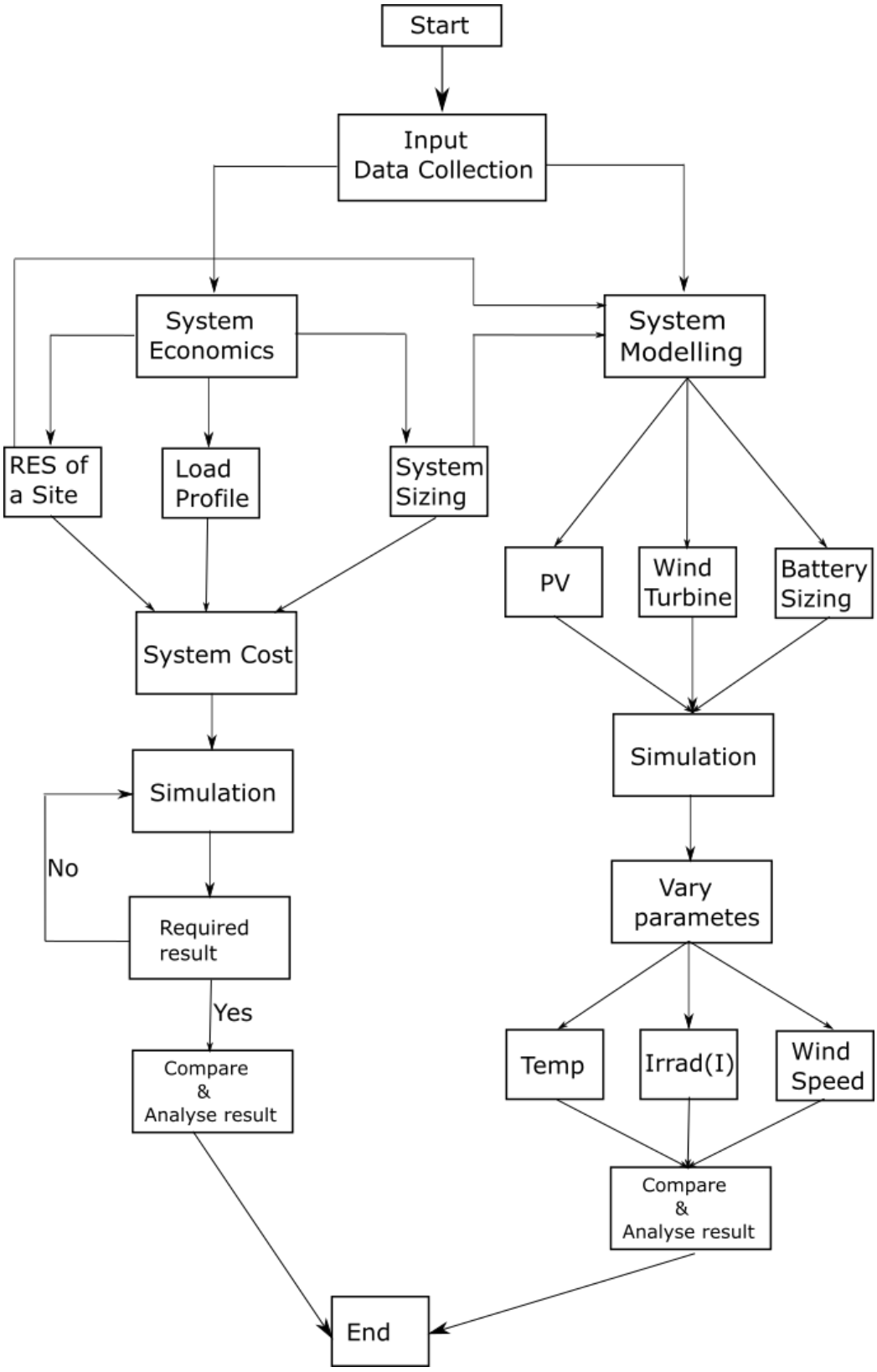

Fig. 3. 2. Flow chart of the project work

In this project, the microgrid generates electricity from photovoltaic systems and small wind turbines, and then energy is stored in batteries to utilize later and balance the system energy flow. According to their demands, the communities obtain enough electricity at a low cost per unit. During the design, adequate equipment was picked. The modeling, analysis, and optimization of a microgrid have been done. Finally, the simulation results and conclusions are analysed. The study is divided into two major categories: cost effectiveness evaluation and system modeling. The HOMER Pro tool is used for cost analysis, while Matlab/Simulink is utilized for modeling.

Sizing the system is essential in this project; sizing is performed on all project components, including the photovoltaic modules, battery controllers, and so on. In designing the system, the photovoltaic array model, wind turbine model, and Battery model existing in Matlab/Simulink are used. The next two parts will address the project's economics and system modeling.

3.2 Data Analysis Techniques

First, the load demand and data collected from the site are applied to the HOMOR Pro software to analyze the economic feasibility of the standalone hybrid microgrid. The sensitivity analysis is carried out. The system modeling and mathematical analysis are then carried out using different techniques to extract the maximum power from the sources using MATLAB/SIMULINK software. In addition, the power electronic converters are designed to control the system and inverter is designed though a PID controller.

3.3 Economic Analysis

It is a fact that the economic development of any a nation is dependent on its energy (especially electrical energy) supply. In this section, renewable energy available on the site is discussed. The load profile is shown, and the sizing of the system is developed. Finally, the cost of components is summarized, then the system economics are analysed.

3.3.1 Renewable Energy Resources of Selected Site

Fig. 3.3 depicts the satellite google map view of the selected location. The renewable energy resources used in this project are solar energy and wind energy resources. This subsection will discuss renewable energy resources available in Dusmareb.

3.3.1.1 Solar Energy Resource

Solar energy resource available in Dusmareb is plenty. The site gets a sun hour of at least 8 hours per day all of the year. The daily solar radiation and clearness index of this site is

collected from NASA Satellite data through HOMER software by entering the latitude and longitude of Dusmareb (5°32.3′ N, 46° 23.2′ E) from Global Solar Atlas data [30].

Fig. 3. 3. Dusmareb city, central Somalia (google map view)

Fig. 3.4. shows the average monthly solar radiation of Dusmareb, which has an annual average of 5.86 kWh/m2/day. As a result of this solar radiation, solar PV modules can be another source of energy generation in this place

.

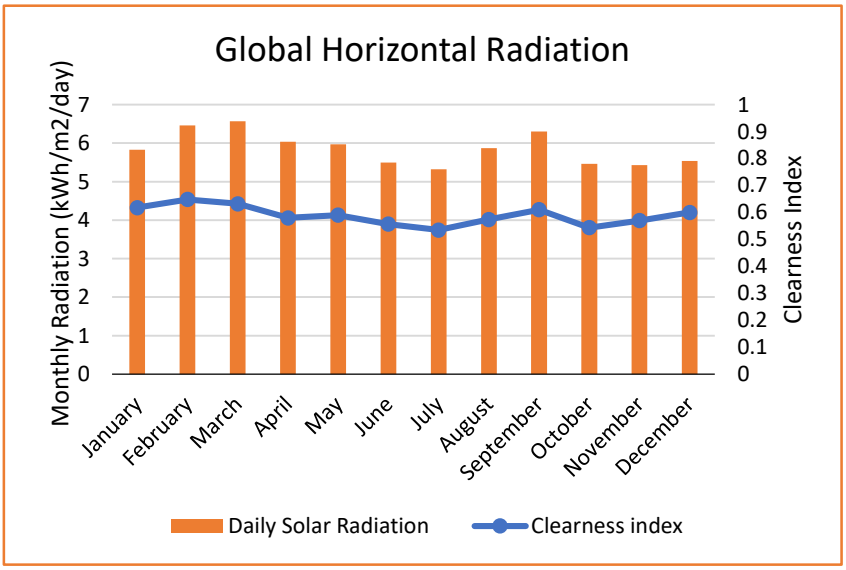

Fig. 3. 4. Dusmareb monthly solar radiation

The best tilt angle to install the solar modules of Dusmareb is 11° south phasing. Nevertheless, in general, the ideal tilt angle of Somalia is 6/180° south phasing. The energy output of solar modules depends on the temperature of the selected place. Dusmareb and generally Somalia has an annual average temperature of 28℃ that is better ideal for solar modules' operating conditions. The monthly temperature of Dusmareb is shown in Fig. 3.5.

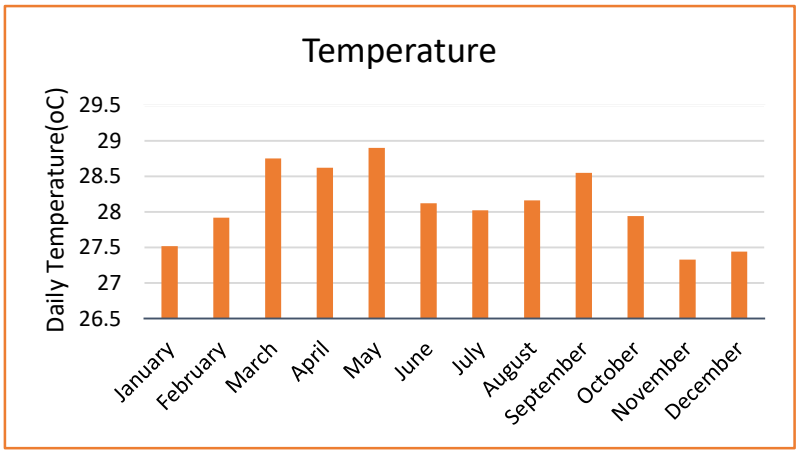

Fig. 3. 5. Monthly average temperature

3.3.1.2 Wind Energy Resource

Wind energy is another source of energy in Dusmareb. The data of wind sources is obtained from NASA satellite data through HOMER software and global wind atlas compiled by the world bank. The wind data of Dusmareb indicates that wind turbines can create electricity. The monthly average wind speed of this location is plotted in Fig. 3.6. The yearly average wind speed of Dusmareb is 6.05 m/s, which is enough to generate a significant amount of electricity.

The wind turbine installed in this area could cover a percentage of the electricity requirement of the city.

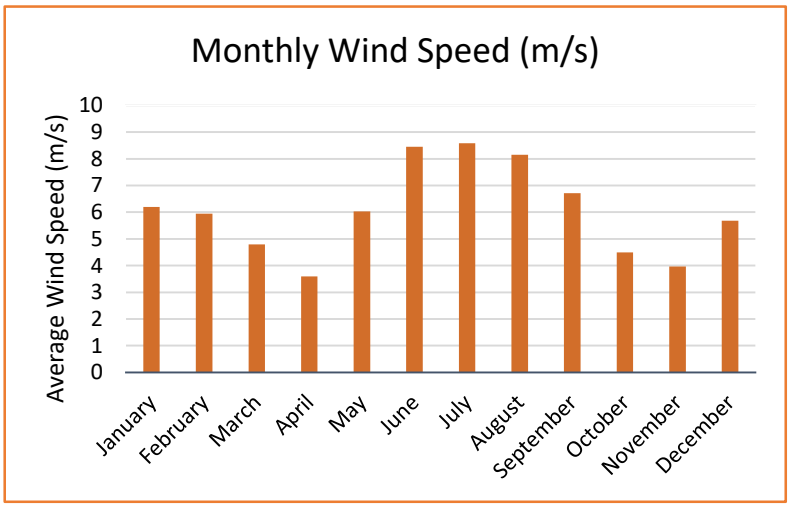

Fig. 3. 6. Monthly wind speed

3.3.2 Energy Demand and Load Profile

The first of such studies of renewable energy sources integration to the power system, the average load profile of electricity is essential. Table 3.1 depicts a typical daily energy usage of

an ordinary residence in urban cities in Somalia. The daily energy consumption is 29.505 kWh/day.

Table. 3 1. Single house daily load consumption

Load	**Watt**	**Hours**	**(Kwh)**
TV And Multimedia	250	12	3
Lighting	300	12	3.6
Refrigerator	150	24	3.6
Washing Machine	450	2	0.9
Blender	300	1	0.3
Laptops	90	2	0.18
Table Fun	25	5	0.125
Electronics	150	12	1.8
Iron	1000	1	1
Other Electronics	1500	10	15
Total (kWh/day)			**29.505**

The characteristics of the daily load profile of 60 households used in this research are displayed in Fig. 3.7. The sample households had average daily energy of 1770.3 kWh/day. Tatal daily power of 73.76 kW and 162.67 kW peak. The load curve demonstrates that the peak hours of energy use are 7 AM to 1 PM. At that moment, business demand and refrigerators in residences are the primary loads.

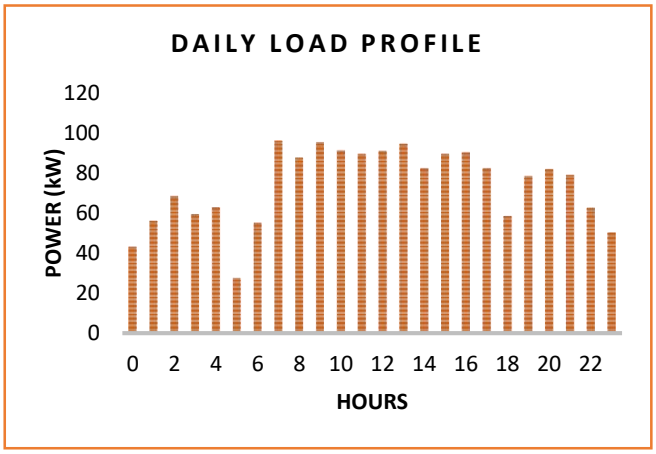

Fig. 3. 7. Daily average load demand

To make the load more realistic, the random fluctuation of a load is preserved day to day 15 percent and time step 10 percent. The peak month is not included because the location proposed to develop this project is always in a nominal state.

3.3.3 Sizing of Standalone Hybrid Systems

This research presents a 200 kWp solar PV system and a 10 kW small wind turbine. This part will discuss the PV modules, which can produce 200 kW of power, and the wind turbine and size of the storage batteries required to store the excess energy for later use. Additionally, the size of the inverter, size of the charge controller, inverter sizing and economic calculation are examined.

The production of Photovoltaic panels is diverse in terms of power, voltage, and current. In this study, Jinko solar panel JKM400-72HL is used. Table 3.2 shows the electrical characteristics of the selected Photovoltaic module. Then, using the 200 kW, the number of modules connected in parallel and the number of modules connected in series can be calculated.

Table. 3 2. Electrical characteristics of selected module

Parameter Name	Value
Maximum power (W)	400.32
Cells per module (Ncell)	144
Open circuit voltage Voc (V)	49.8
Short-circuit current Isc (A)	10.36
Voltage at maximum power point Vmp (V)	41.7
Current at maximum power point Imp (A)	9.6
Temperature coefficient of Voc (%/deg.C)	-0.34
Temperature coefficient of Isc (%/deg.C)	0.0630012
Length	2,008mm (79.1in)
Width	1,002mm (39.4in)
Weight	22.5kg (49.6lb)

3.3.3.1 PV Modules and PV Area Calculation

The required peak power calculated of the system and the DC bus bar voltage usually taken to be a multiple of the nominal battery voltage of 12 V should be considered to calculate the number of modules in series and parallel.

$$\mathrm{I}_{system} = \frac{Peak\ Power}{V_{system}} \tag{3.1}$$

$$= \frac{200 \times 10^3 W}{400} = 500\ \mathrm{A}$$

Where I is system current, and V is system voltage selected as load requirement of the location. The number of parallel and series modules needed to get the above-calculated current can be found through equation 3.2 to 3.4.

$$N_{paralel} = \frac{\mathrm{I}_{system}}{I_{module}} \tag{3.2}$$

$$= \frac{500\ A}{9.6} = 52.08 \cong 52\ modules$$

$$N_{series} = \frac{\mathrm{V}_{system}}{V_{module}} \tag{3.3}$$

$$= \frac{400\ A}{41.7} = 9.592 \cong 10\ modules$$

$$N_{total} = N_{series} \times N_{paralel} \tag{3.4}$$

$$= 10 \times 52 = 520\ modules.$$

Where $N_{paralel}$ = number of PV modules connected in parallel.

I_{moduel} = Maximum operating current of the chosen module.

N_{series} = number of PV modules connected in series.

V_{system} = DC bus bar voltage of the system.

V_{module} = maximum operating voltage of the chosen module.

N_{total} = total number of modules.

The area needed to install PV panels may be determined. There are various ways to be calculated. The width and length of one module indicated in table 2 are used in this scenario.

$$area\ of\ one\ module = \text{length} \times \text{width} \tag{3.5}$$

$$= 2.008\text{m} \times 1.002\text{m} = 2\ m^2$$

$$T_{area} = \text{area of one module} \times N_{total} \tag{3.6}$$

$$= 2\ m^2 \times 520 = 1{,}040\ m^2$$

3.3.3.2 Sizing of Wind Turbine

In this study, a generic 10 kW wind turbine is utilized in the HOMER Software to examine the system's viability, and a 10 kW wind turbine is modelled in Matlab/Simulink. Table 3.3 displays the wind turbine characteristics obtained from Matlab software. The following parts will go over how to model a whole system.

Table. 3 3. Characteristics of wind turbine model used in matlab/Simulink

Wind Turbine Parameter	Parameter value
Base wind speed (m/s)	6-12
Nominal mechanical output power (W)	10 kW
Base power of the electrical generator (VA)	11.1 kVA
Per unit of nominal mechanical power	0.8
Per unit of base generator speed	1
Pitch angle beta to display wind-turbine power characteristics (deg)	0

3.3.3.3 Battery Sizing

A standalone hybrid system should have a storage system since the generation sources are not generating continuous power every time.

In the present work, the lead-acid battery is utilized to store the access energy generator in a day to use in a night. Table 3.4 illustrates the parameters of the used battery than flowed by sizing of the battery capacity.

When sizing the battery, the daily energy demand, efficiency of a chosen battery, the depth of discharge, and days of autonomy which are the number of days that the battery can supply the load without any support from generation sources of a chosen battery, should be considered.

Table. 3 4. Battery parameters

Name	Value
Nominal Voltage (V)	12
Maximum Capacity (Ah)	260
Efficiency (%)	85
Day of autonomy	2
Depth of Discharge (DOD)(%)	80

$$E_{battery} = \frac{\mathrm{E}_{demand} \times days\ of\ autonomy}{B_{efficiency} \times DOD \times Vb_{nominal}} \quad (3.7)$$

$$= \frac{1770.3 \times \frac{10^3 \mathrm{Wh}}{\mathrm{day}} * 2}{0.85 \times 0.8 \times 12\ \mathrm{V}} = 433897.0588\ \mathrm{Wh/day}$$

$$B_{\mathrm{Capacity}} = \frac{E_{battery}}{\mathrm{V}_{system}} \quad (3.8)$$

$$= \frac{433897.0588}{400} = 1084.742\ Ah$$

Now the number of batteries connected in parallel or in series can be calculated using the flowing formulas.

$$B_{\mathrm{parallel}} = \frac{B_{\mathrm{Capacity}}}{maximum\ capacity} \quad (3.9)$$

$$= \frac{1084.742}{260} = 4\ batteries$$

$$B_{\mathrm{series}} = \frac{V_{\mathrm{system}}}{nominal\ voltage} \quad (3.10)$$

$$= \frac{400}{12} = 34\ batteries$$

So the total required batteries, $B_{\mathrm{total}} = B_{\mathrm{parallel}} \times B_{\mathrm{series}}$ (3.11)

$$= 4 \times 34 = 136\ batteries.$$

3.3.3.4 Charge Controller Sizing

Charge controllers prevent battery overcharging and also prevent the batteries from sending their charge back through the system to the charging source. The size of the charge controller based on the maximum charge current of the solar array and the rated current of the charge controller. [31]

$$current\ controller\ rating = 1.25 \times I_{sc} \times N_{paralel} \quad (3.12)$$

$$= 1.25 \times 10.36 \times 52 = 673.4\ \mathrm{A}$$

As a result, a 12V, 60Ah MPPT-based solar charge controller was selected from the specifications based on the present controller rating values. Equation 3.13 can now be used to calculate the number of charge controllers.

$$number\ of\ charge\ controllers = \frac{current\ controller\ rating}{one\ controller\ current\ rating} \quad (3.13)$$

$$= \frac{673.4}{60} = 11$$

3.3.3.5 Inverter Sizing

The inverter's size must be determined by its ability to manage the estimated maximum power of the AC load. As a result, a power factor of 25-30% larger than the total AC rated power should be considered [32]. The rated power of the inverter becomes 200000 W + (0.28 × 200000) = 256000 W, therefore the selected inverter is The Hybrid SMA inverter SMA Tripower 10.0, and the inverter is 15 KW, which can operate at the photovoltaic system's continuous nominal power. Therefore, the number of inverters can be calculated.

$$number\ of\ inverters = \frac{rated\ power\ of\ the\ inverter}{rated\ power\ of\ one\ inverter} \quad (3.14)$$

$$= \frac{256000}{15000} \cong 18\ inverters$$

3.3.4 System Cost

The primary criterion for selecting power system components in this Project is cost, as the primary objective of the study is to determine the optimal power system configuration that meets demand while minimizing NPC and LCOE [33]. The net present value of energy and the cost of energy are the two most critical indicators of the economic behaviour of renewable energy systems [7]. The HOMER simulation requires the economic input parameters for this design, including the annual real interest rate and project lifetime. The expected life of the power plant is 25 years, and the discount rate is 8% the inflation rate is taken as 2%. The following section discusses the cost estimation of the hybrid standalone microgrid system, along with its specifications.

- The system's capital cost (initial cost) is high.
- The expense of maintenance is minimal.
- There is no expense for fuel.
- Costs of replacement are low.

3.3.4.1 Capital Investment Costs

The initial capital cost of equipment comprises the cost of photovoltaic modules, wind turbines, batteries, and inverters [34]. The table 3.5 below summarizes the components' initial investment costs.

Table. 3 5. Initial capital cost of hybrid system main components

Component Name	Initial Cost
PV Panels	$104000
Batteries	$19040
Inverter	$67,964.4
Charge Controller	$2860
Wind Turbine	$50,000

Where 0.5$/W in PV panels that is $0.5 \times 400 \times 520 = \$104{,}000$. Single Battery costs $140, so 136 battery cost $136 \times \$140 = \$\$19040$. One 15kW inverter costs $3775.8, so 18 inverters cos $18 \times 3775.8 = \$67{,}964.4$. Each piece of charge controller costs $260, so 11 pcs cost $11 \times 260 = \$2860$. The cost of 10 kW wind turbine is between $30,000 to $50,000 as market [35].

3.3.4.2 Costs of Operation and Maintenance (O&M)

It is the expense associated with the system's maintenance and operation. The total cost of operation and maintenance of the scheme components evaluated in this project varies. Wind power O&M costs are extremely inexpensive in comparison to other types of power facilities [36]. The flowing formula is used to calculate the operation and maintenance cost.

$$\text{O\&M Cost of PV Panels} = 2\%\text{PV} \times \frac{1+i}{1+d} \times \left[\frac{1-\left(\frac{1+i}{1+d}\right)}{1-\left(\frac{1+i}{1+d}\right)}\right]^{n} \qquad (3.15)$$

The operation and maintenance cost of a wind turbine is almost negligible, so in this project, zero is taken.

3.3.4.3 Cost of Replacement:

This is the expense of replacing worn-out components at the end of their useful life.

This cost is different from the component's initial cost for the following reasons. At the conclusion of the component's lifecycle, not all of the component's spares must be replaced. The equation 3.16 is used for calculating the replacement cost.

$$\text{Placement Cost} = \text{Ai}\left(\frac{1+\text{i}}{1+\text{d}}\right)^{n} \quad (3.16)$$

Where

Ai is the initial cost of an equipment.

i is the inflation rate, taken 2%

d is the discount rate, taken 8%

n is the life time of the project.

Battery life is estimated to be five years, which means it should be replaced five times during the project's lifespan. The cost of battery replacement is calculated for the first time after five years, the second time after ten years, the third time after fifteen years, the fourth time after twenty years, and finally the fifth time after twenty-five years, as follows.

For installation cost 10% of PV panel initial cost and 5% of wind turbine.

Net present value (NPV) the Hybrid standalone microgrid system can be calculated by using the equation 3.17.

$$\text{NPV} = PV_c + Batt_c + Inv_c + Chcont_c + WT_c + TO\&M_c + TRe_c + TInst_c \quad (3.17)$$

The annual cost of the system is also calculated using equation 3.18.

$$\text{TA}_{Cost} = \text{NPV} \times \left[\frac{\text{i} \times (\text{i}+1)^{n}}{(1+\text{i})^{n}-1}\right] \quad (3.18)$$

Levelized Cost of Electricity (LCOE) can be found the flowing equation.

$$LCOE = \frac{\text{TA}_{Cost}}{365 \times E_{demand}} \quad (3.19)$$

3.4 System Modelling

3.4.1 Photovoltaic Model

This work uses the existing model of The PV array in the Matlab/Simulink. The characteristics of the model are considered under variation of solar radiation and temperature. The mathematical concept of solar photovoltaic is discussed in chapter 2. Fig. 3.8. illustrates the existing PV array in Simulink. There are two inputs solar radiation and temperature. In the output, the measurement (M) can be measured the output current and voltage. The current and power characteristics of the selected modules by varying the irradiation from 100 $\text{W/m}^2$to 1000 W/m^2 are shown in Fig. 3.9. This illustration's title indicates the number of series and parallel modules and the name of the chosen photovoltaic module. The maximum power at 200 kW can be found when the maximum operating voltage is 417 V and irradiance is 1kW/m^2.

Current increases as the irradiance increases. Therefore, short circuit current is directly proportional to the irradiance, while the variation of voltage is much smaller and is usually neglected in practical applications[11], [37].

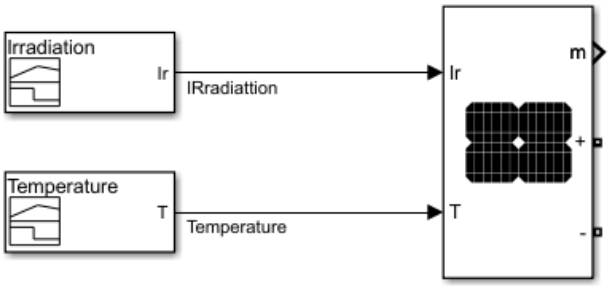

Fig. 3. 11. Simulink model of solar PV array

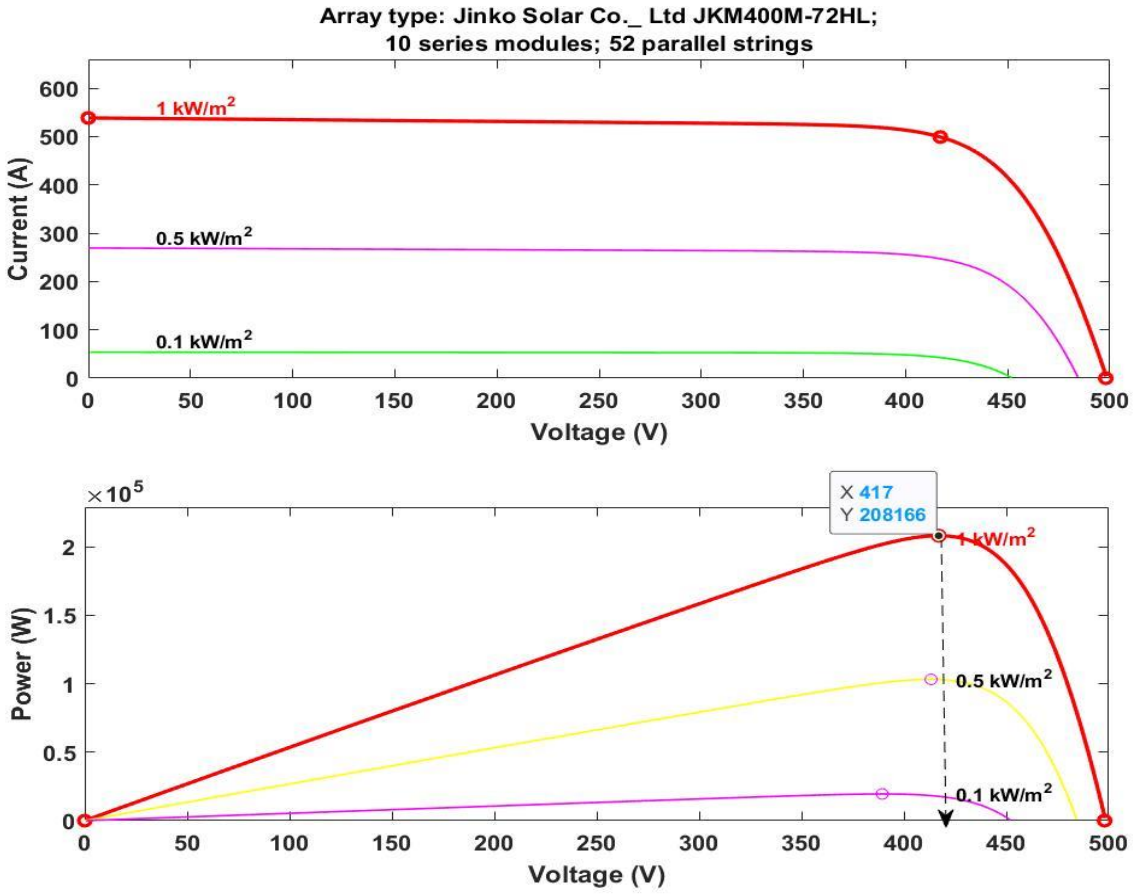

Fig. 3. 12. I-V and P-V characteristics of photovoltaic array by varying solar irradiation

Irradiation is not the only environmental factor that influences the solar array. Another factor that influences the Solar PV Array is the temperature. Fig. 3.10. The P-V characteristics of the chosen module are displayed by adjusting the temperature from 25°C to 60°C. Voltage drops as the temperature rises. As a result, the temperature has a greater impact on voltage.

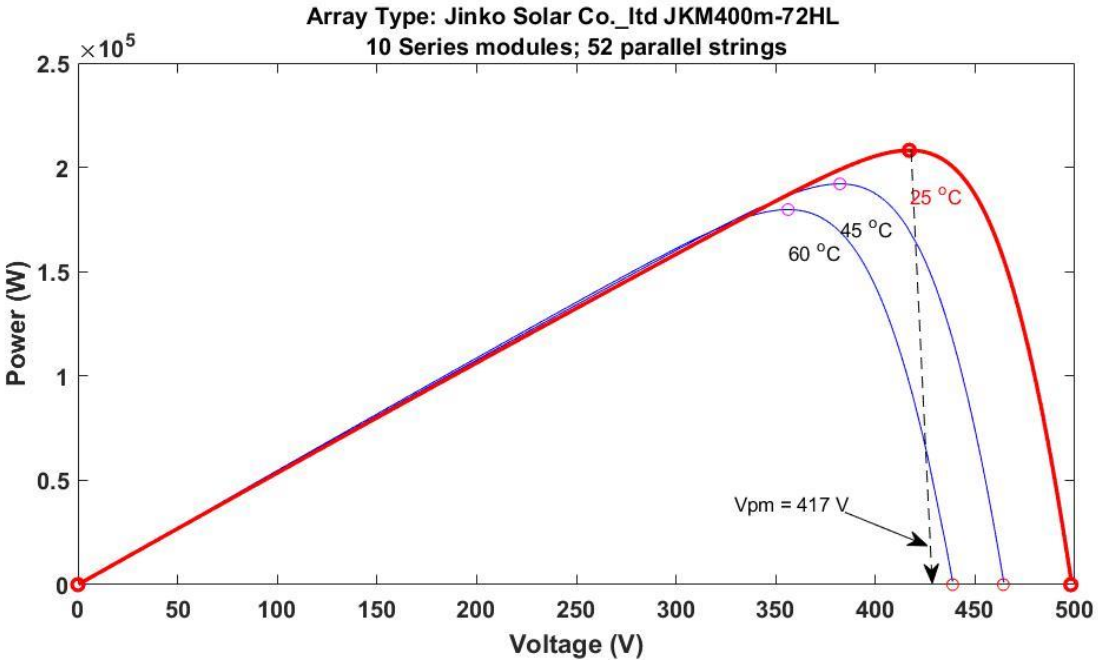

Fig. 3. 13. The effect of temperature on P-V characteristics of PV array

3.4.2 Boost Converter Modelling

In general, DC-DC converters are power electronic converters that regulate the voltage. The main functionality of DC-DC converters is to step up or step down the voltage. As the output voltage of solar photovoltaic varies, the boost converter is used to step voltage and track the maximum power. The configuration of the boost converter is illustrated in Fig. 3.11 [38].

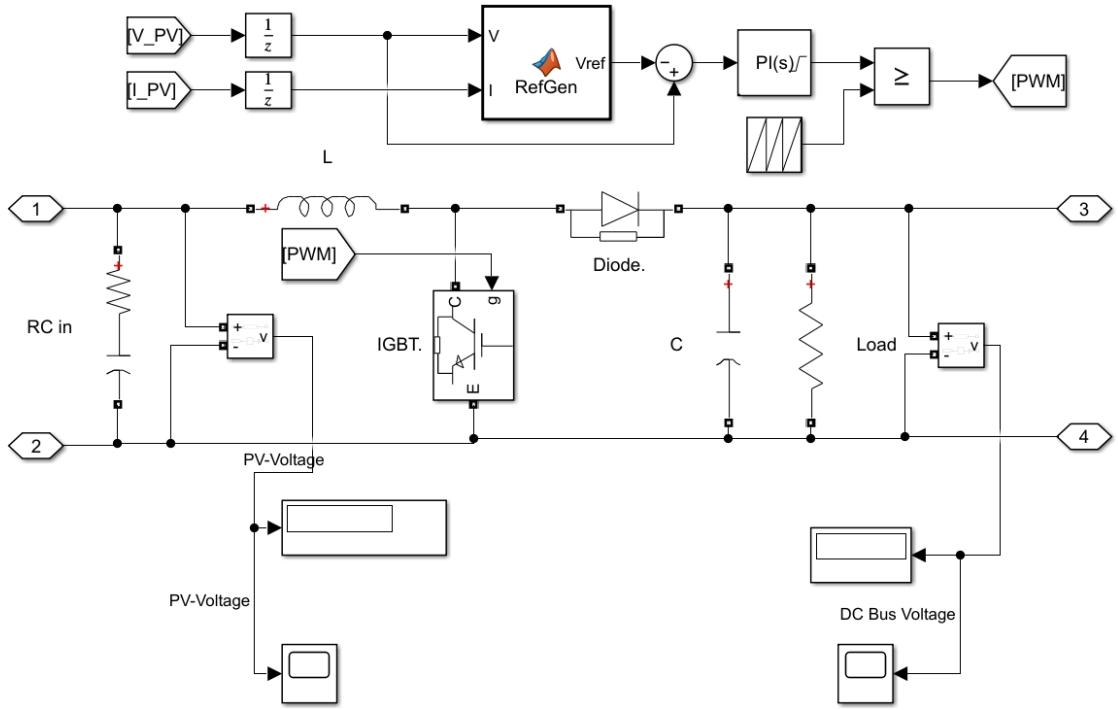

Fig. 3. 14. Simulink model of boost converter with MPPT

The RCin is used to prevent the sudden change of PV array output. The mathematical equations for the boost parameter were determined using the following Equations.

$$L = \frac{[PV_{voltage} \times (DC_{bV} - PV_{voltage})]}{F_s \times \Delta I \times DC_{bV}} \quad (3.20)$$

$$C = \frac{[I_{Bus} \times (DC_{bV} - PV_{voltage})]}{F_s \times \Delta V \times DC_{bV}} \quad (3.21)$$

In this project, the reference DC bus voltage is 400V, the DC voltage ripple is taken as 1% of DC bus voltage, so 1% of 400V is 4V, and the switching frequency is 5 kHz.

MATLAB CODE OF PERTURBE AND OBSERVE METHOD

```
function Vref = RefGen(V, I)
Vrefmax = 498;
Vrefmin = 0;
Vrefinit = 400;
deltaVref =0.5;
persistent Vold Pold Vrefold;

dataType = 'double';

if isempty(Vold)
    Vold = 0;
    Pold = 0;
    Vrefold = Vrefinit;
end

P = V*I;
dV= V-Vold;
dP = P-Pold;

if dP ~=0
    if dP <0
        if dV<0
            Vref= Vold - deltaVref;
        else
            Vref = Vold + deltaVref;
        end
    else
        if dV<0
            Vref=Vrefold + deltaVref;
        else
            Vref= Vrefold - deltaVref;
        end
    end
else Vref = Vrefold;
end
if Vref>=Vrefmax | Vref<= Vrefmin
    Vref = Vrefold;
end
Vrefold = Vref;
Vold = V;
Pold = P;
```

Fig. 3. 18. P & O method code

The current ripple is 5% of the DC bus current that becomes 25.64 A. The Appendix A.1 shows Matlab Code for calculating this values. Now, we can calculate the values of inductance (L) and capacitance (C). $\mathrm{L} = \frac{[390(400-390)]}{5000\times25.64\times400} = 76\mu H, \mathrm{C} = \frac{[513(400-390)]}{5000\times4\times400} = 625\mu F$ The boost converter gate is controlled by a maximum power point tracking mechanism. The perturb and observe MPPT mechanism is employed in this research. The RefGen block's Matlab code is shown in Fig.3.12. The MPPT algorithm is based on the fact that at maximum power, the output power (P) derivative for the panel voltage (V) is equal to zero. Various MPP algorithms are available in the literature to improve photovoltaic system performance by effectively tracking the MPP.

3.4.3 Wind Turbine

Wind turbine, control method, generator, and power converter make up the Wind Energy Conversion System (WECS). The conversion process employs a variety of generators, including the Double Fed Induction Generator (DFIG) and the Permanent Magnet Synchronous Generator (PMSG) (PMSG). Because of its high efficiency and controllability, the PMSG is widely used in WECS. Permanent magnet materials with high coercive field strength, temperature resistance, and low cost are becoming increasingly popular for wind energy generation. [39].

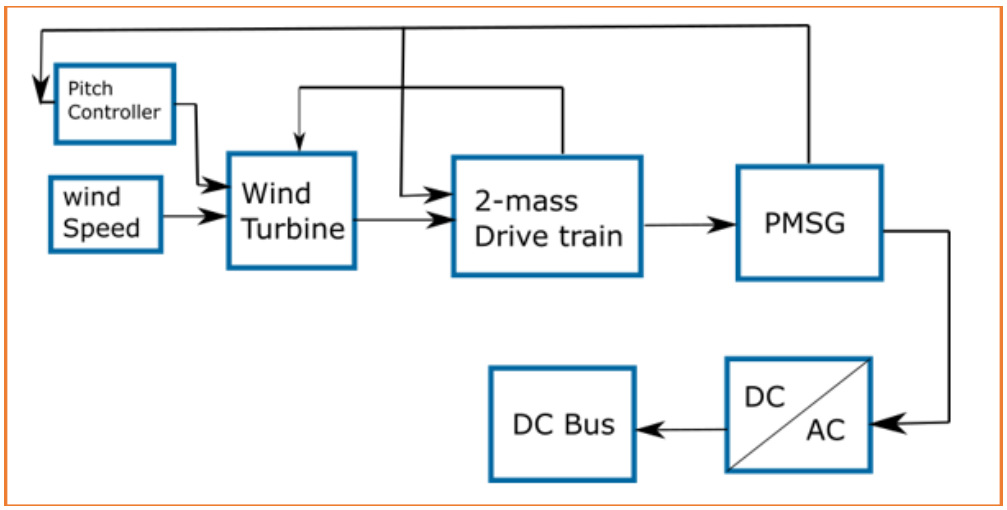

Fig. 3. 19. Block diagram of WECS

Fig. 3.13. depicts the block diagram of the wind energy conversion system used in this project. The power characteristics of a wind turbine are shown in Fig. 3.14 when the pitch angle is zero.

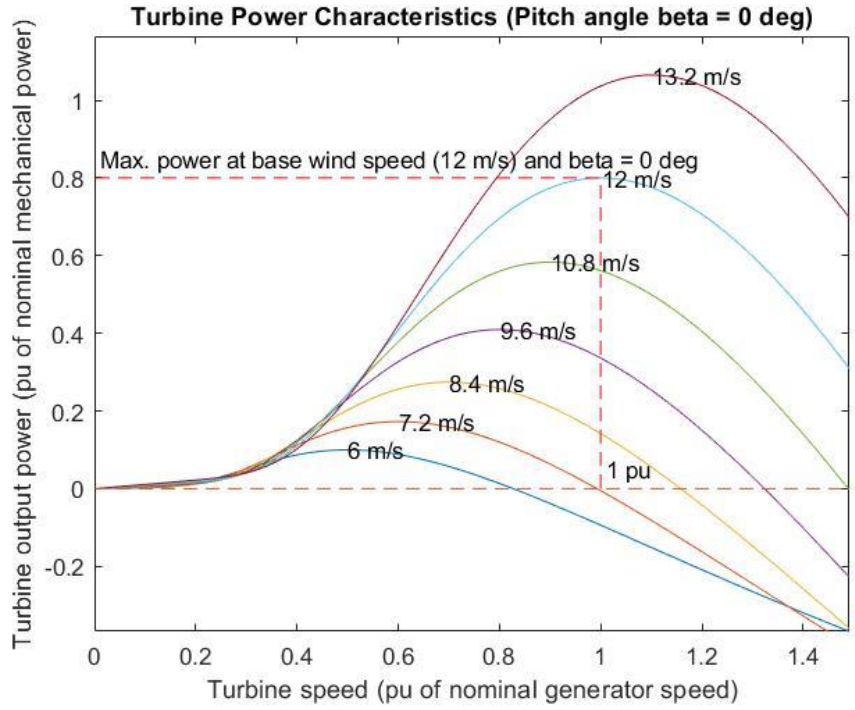

Fig. 3. 20. Power characteristics of a wind turbine

The drive train of a wind turbine is the mechanical system that includes the turbine, generator, and gearbox. The gearbox converts the wind turbine's low speed into the desired generator turbine speed. The following is the mathematical model of a two-mass drive train: [40].

$$2\mathrm{H}\frac{dw_t}{dt} = T_m - T_e \tag{3.22}$$

$$\frac{1}{w_{ebs}}\frac{d\theta_{sta}}{dt} = w_t - w_r \tag{3.23}$$

$$T_s = K_{ss}\theta_{sta} + D_t\frac{d\theta_{sta}}{dt} \tag{3.24}$$

where,

Ht = Inertia constant of the turbine

θsta = Shaft twist angle

wt = Angular speed of the wind turbine

wr = Rotor speed of generator

$webs$ = Electrical base speed

Ts = Shaft torque

Kss = Shaft stiffness

Dt = Damping Coefficient

The Simulink model of wind energy conversion system given in Fig. 3.15. Connection port shown is used to connect the common DC bus.

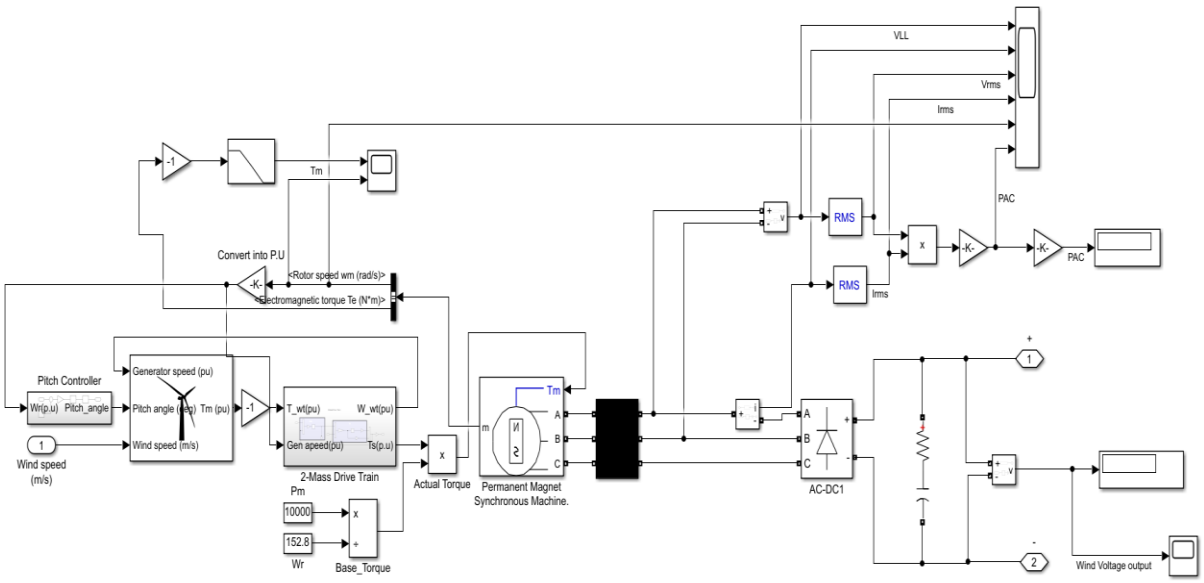

Fig. 3. 24. The Simulink model of a wind turbine system

3.4.4 Bidirectional Converter and Storage Battery

The battery is an integral component of the standalone microgrid hybrid system because of the intermittency of the photovoltaic array and wind turbines [7]. A battery is a power storage device that saves excess power and uses it to power the load and generators when they are needed. The PV and wind energy systems (detailed in the preceding sections) are linked to a constant voltage DC bus. The DC bus is also connected to the battery bank. This constant voltage DC bus is used for all power transfers, whether from generators to battery banks, generators to loads, or battery banks to loads. Because the power flow associated with the battery is not unidirectional, a bidirectional converter is necessary to charge and discharge the battery in times of excess and scarcity of electricity [41]. Bi-directional DC-DC converters are so named because, depending on the application, they enable power to flow in both directions. The bidirectional converter has many applications, including hybrid cars and uninterruptible power supply (UPS), fuel cell storage systems, and renewable energy systems. Fig. 3.16. shows the MATLAB/SIMULINK Model of the DC-DC bidirectional connected with the battery. The calculation of a parameter's value can be done using the following formula.

$$\mathrm{L} = \frac{[V_{bout}(V_{bin} - V_{bout})}{F_s \times \Delta I \times V_{bin}} \tag{3.25}$$

$$\mathrm{C} = \frac{\Delta I}{8 \times F_s \times \Delta V} \tag{3.26}$$

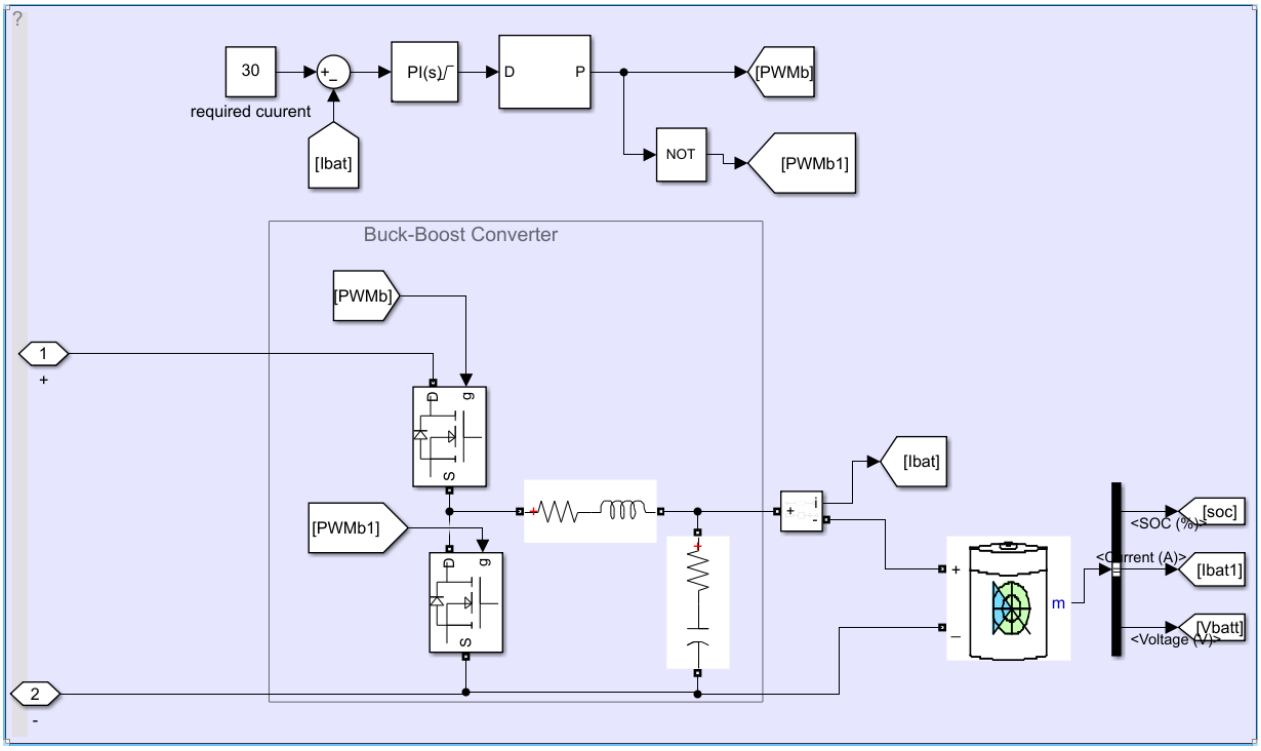

Fig. 3. 28. Bidirectional and battery Simulink model

3.4.5 Inverter

The photovoltaic system output is direct current, whereas the WECS output has already been converted to direct current using a rectifier to make the system controllable. The direct current bus link connects all generating sources and storage systems. The majority of loads are alternating current loads, necessitating the need of an inverter to convert the DC link bus to alternating current. An inverter is a type of electronic device that converts direct current to alternating current. As illustrated in Fig. 3.17, The study designs an IGBT based on an inverter with current and voltage controller pulse width modulation. The voltage and current controllers employ a PID controller, which improves the system's dynamic response and minimizes errors. As illustrated in fig. 26, a reference voltage of 400 V is used. Vabc and Iabc are converted from an inverter to park transformation dq0 via the transformation system. The voltage controller compares the reference voltage to Vd and Vq, whereas the current controller uses Id and Iq to generate a PWM signal, which is then converted to ABC to provide the switch gate. Finally, because the inverter generates three-phase voltage and three-phase current with harmonics, the RLC filter is employed to remove the harmonics before supplying the AC loads.

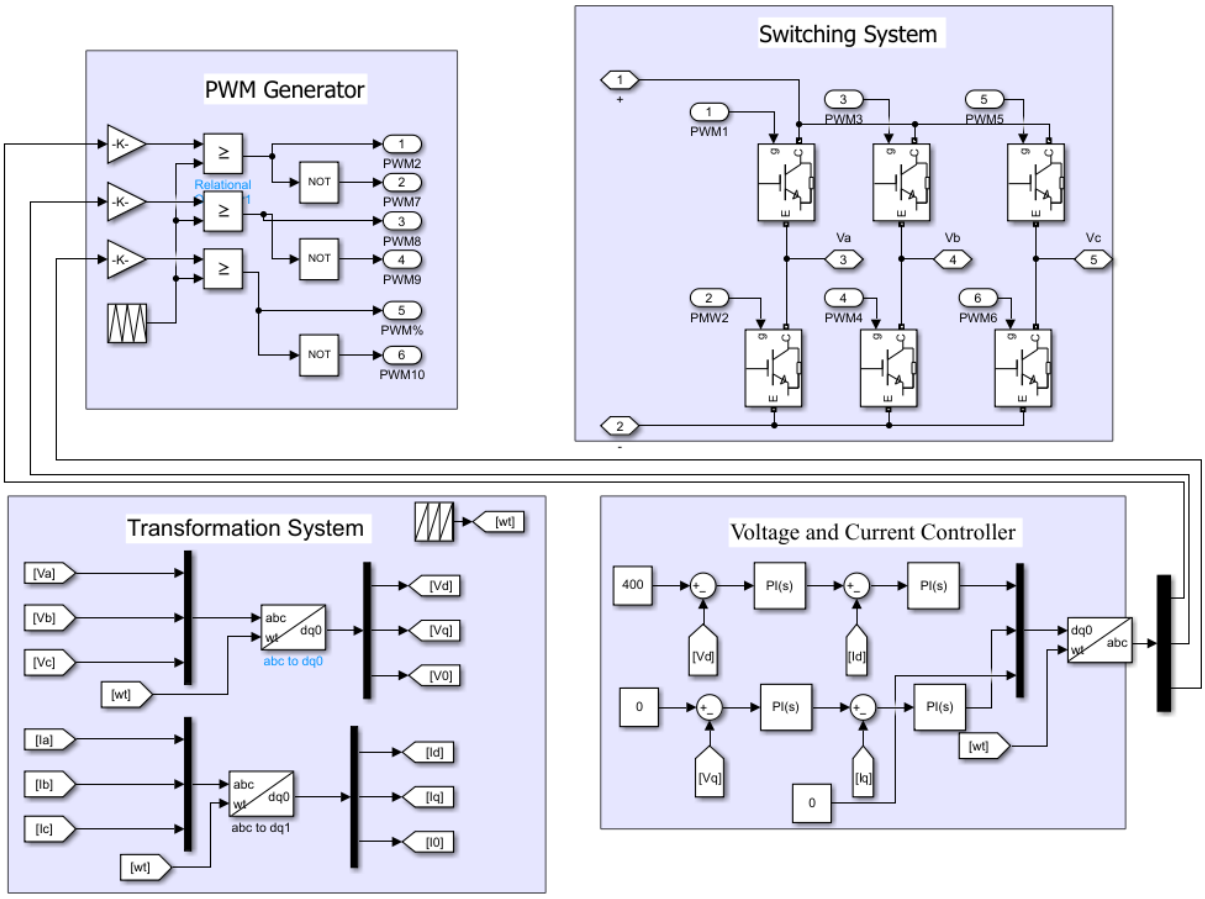

Fig. 3. 29. Simulink model of an inverter

3.4.6 Model of a Hybrid Microgrid System in MATLAB/SIMULINK

The preceding sections covered the components of a hybrid standalone Microgrid system. The overall comprehensive design of the system is shown in Fig. 3.18

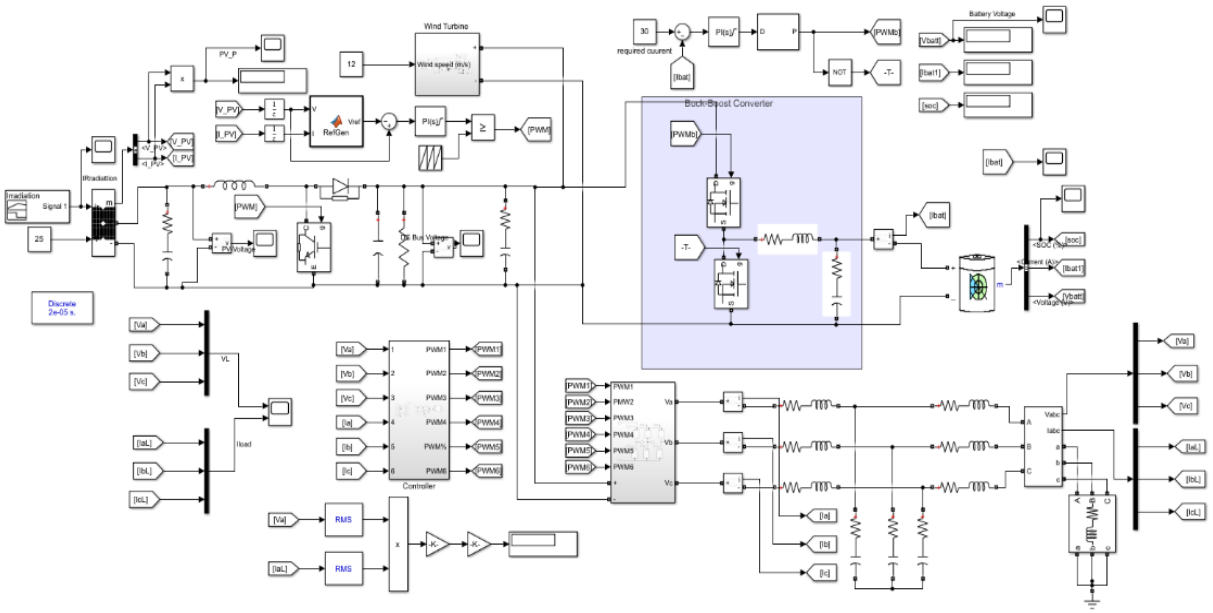

Fig. 3. 30. Overall System Modelling in Simulink

CHAPTER 4

Simulation Result and Analysis

4.1 Introduction

This chapter discusses the results of the hybrid cost-effective standalone system. The optimization result from HOMER Software will be displayed together with its sensitivity, and then the outcome will be analysed. Following that, the Matlab/Simulink simulation result will be displayed and examined.

4.2 HOMER Pro Model

Fig. 4.1. illustrates the hybrid islanded microgrid modelled using HOMER Pro software. The designed system consists of photovoltaic solar, wind turbine, battery, interface inverter and loads.

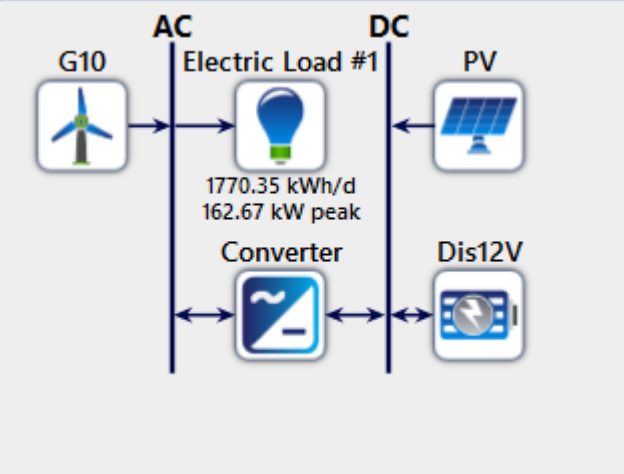

Fig. 4. 1. HOMER diagram for the system architecture

4.2.1 Result from HOMER Pro Simulation

The first result of the system simulation in HOMER Pro software is an optimization result. Optimization results are divided into two categories: categorized and overall. In this project, the categorized result is used because it is the most optimized output. The system's net present value is $1,277,844, and the Levelized Cost of Electricity (LCOE) is 0.153$/kWh as a result. The proposed LCOE for the project is about a fourth of what the Dusmareb community currently pays, which is 0.6$/kWh. The system's monthly power generation and storage are depicted in Fig. 4.2.

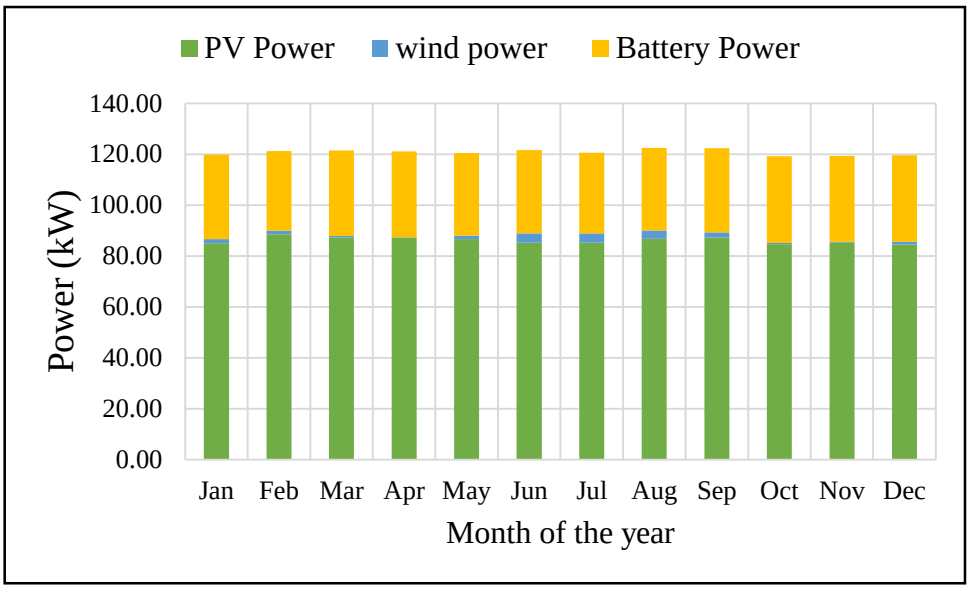

Fig. 4. 2. Monthly electricity production

As shown in the photovoltaic system generates most part of the electricity around 98%, while battery stores the excess generated power and supply to the system when it needed. The wind turbine generates the rest 2% percent of the electricity. Excess electricity is approximately 2.37 percent, which is quite low, indicating that the system is sufficiently efficient. Fig. 4.3 indicates the monthly electricity generation included excess energy generated.

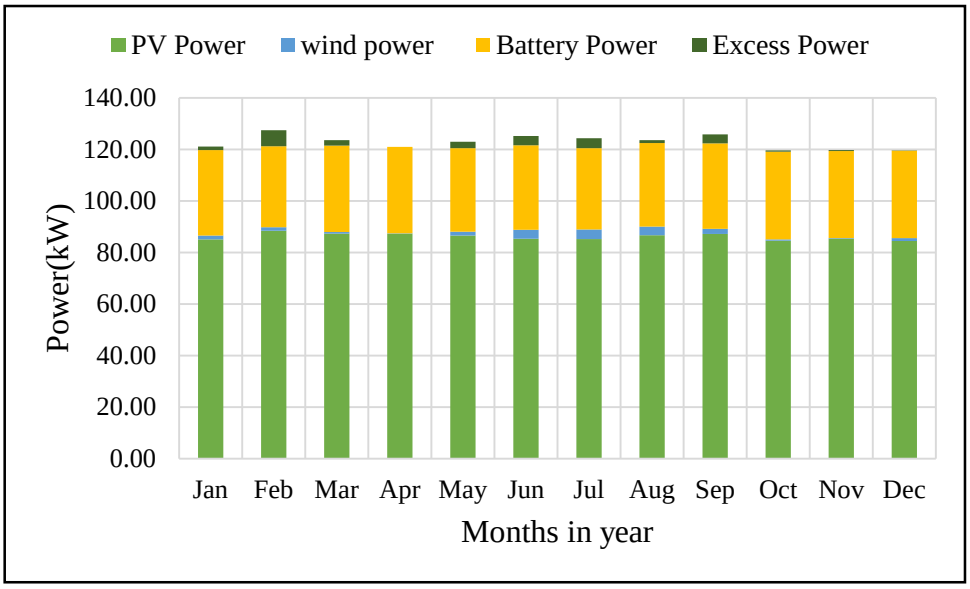

Fig. 4. 3. Total electricity generation with excess power

As the generation sources are renewable energy sources, the system emits no emissions. Continuous supply of a load demand is key issue of the work, Fig. 4.4 shows how the generation sources and their storage system satisfies load demand in first seven days of January. To

illustrate more closely the one-day load supply is plotted in Fig. 4.5. The HOMER Pro results indicate that the suggested hybrid standalone microgrid system is cost-effective at the study location.

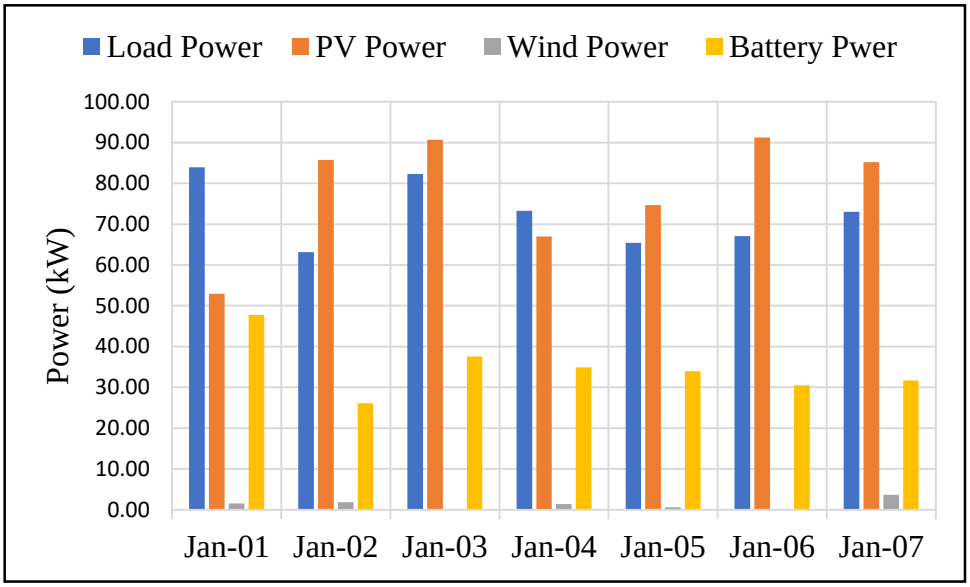

Fig. 4. 4. Load demand and power generation

On the other hand, because the wind turbine generates a negligible quantity of electricity in this system and its installation is technically challenging and requires expertise, we can install the standalone photovoltaic system. As previously stated, the cost of electricity in Somalia is extremely expensive, and so the exploitation of renewable energy is the most cost effective in terms of energy and the environment.

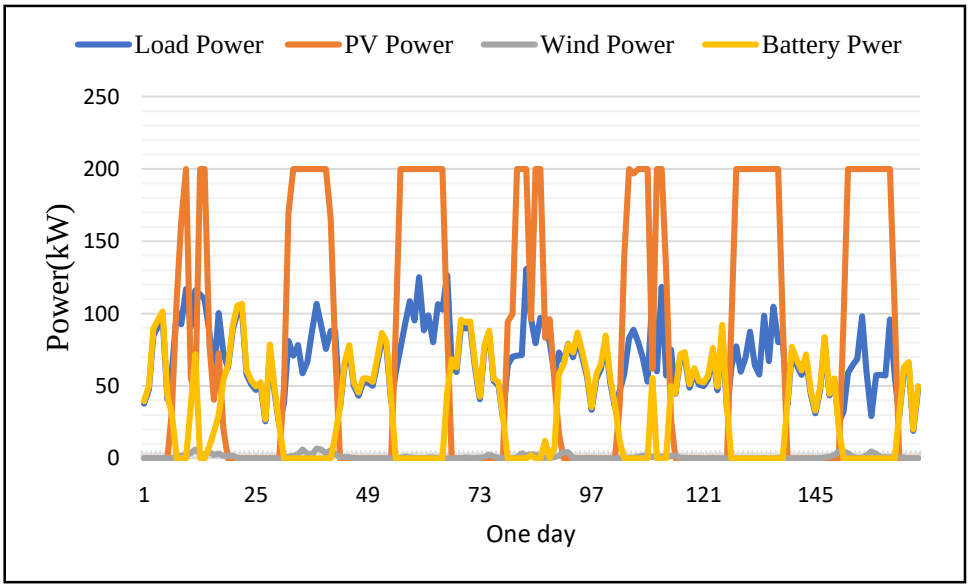

Fig. 4. 5. Load power system power

The net present values of the proposed system after the optimization is illustrates in Fig. 4.6

the photovoltaic system carries 59% of the total net present values of the system, while batteries are second.

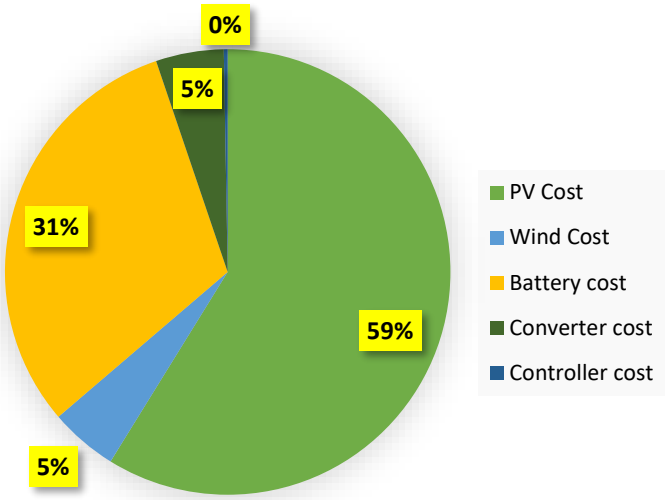

Fig. 4. 6. NPV of the system components

4.3 Matlab/Simulink Result

The Matlab/Simulink simulation for this project is divided into different parts. In the first stage, the photovoltaic system is simulated under various irradiation conditions. The irradiance is increased from 0.1 to 1 kilowatts per square meter. The change in irradiation is depicted in Fig. 4.7. As illustrated in Fig. 4.7, the MPPT system operates properly during irradiance changes and monitors the maximum power at irradiation.

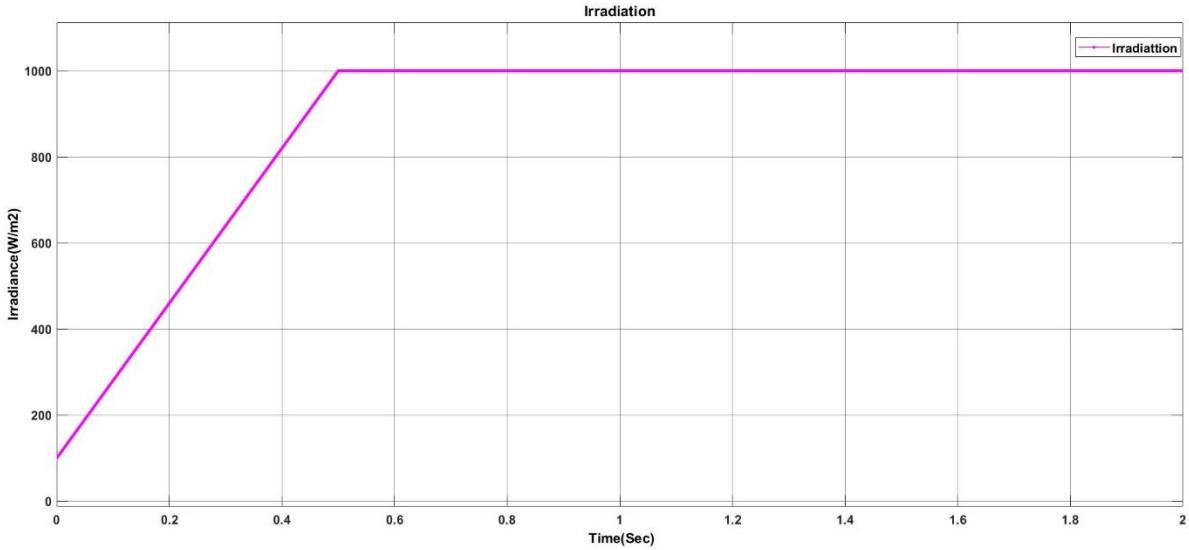

Fig. 4. 7. Variation of an irradiation with time

The maximum power point tracking strategy employed in this research is perturb and observe method, the Fig. 4.8 reveals that the maximum power flows the change of irradiance.

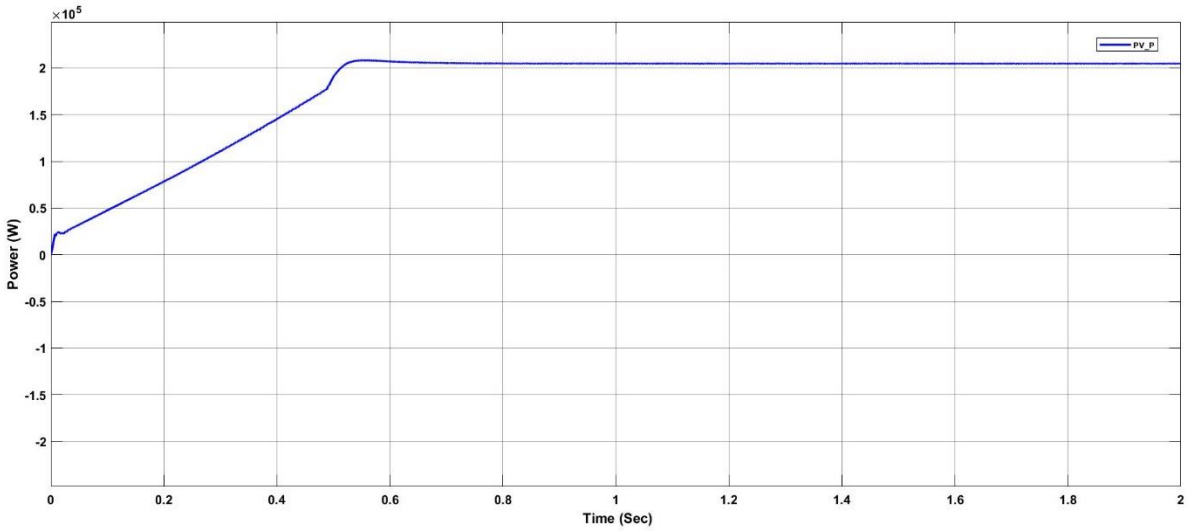

Fig. 4. 8. PV-power output at MPPT

Fig. 4.9 shows the photovoltaic system's output voltage; the voltage can be as low as 350 V, but as irradiance increases, the system's output voltage increases.

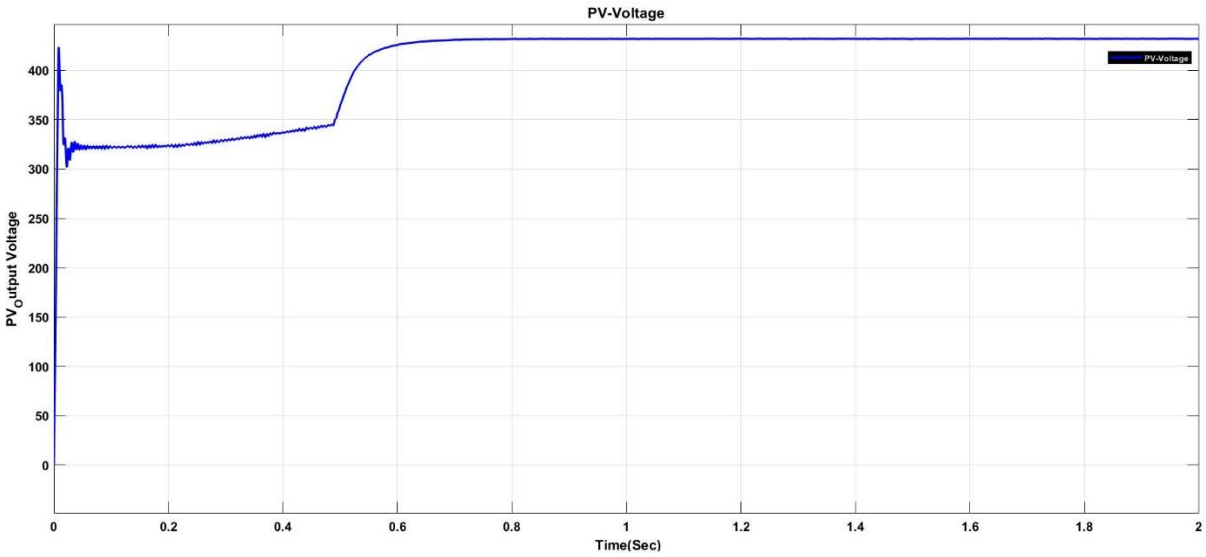

Fig. 4. 9. Output voltage of PV

The second stage simulates a wind turbine and generates alternating current, voltage, and power. The output of an AC wind turbine is represented in Figs. 4.10 to 4.13, and then converted to a DC system via an AC to DC rectifier in order to incorporate the photovoltaic system at the DC link bus. The fig. 38 illustrates the DC voltage generated by a wind turbine.

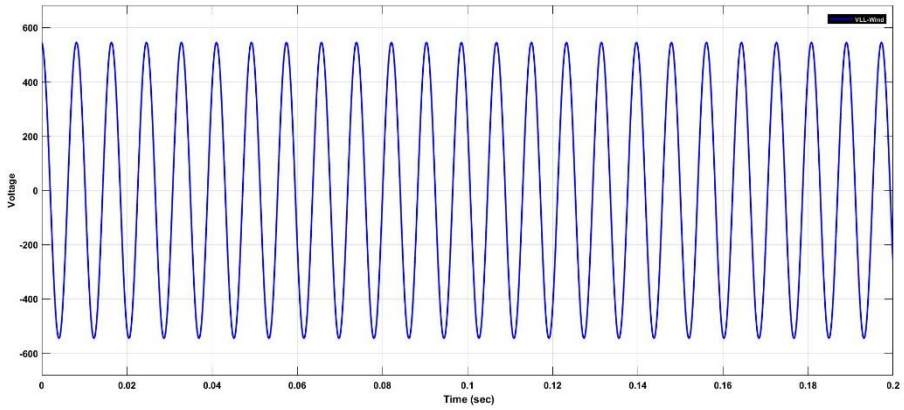

Fig. 4. 10. Wind turbine AC output voltage

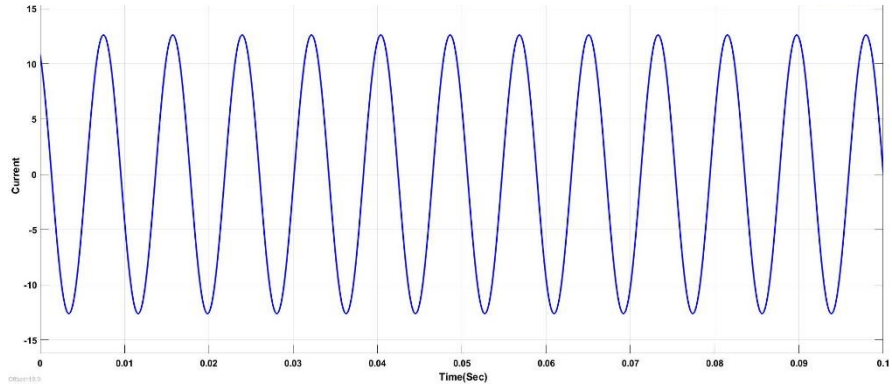

Fig. 4. 11. Wind turbine output current

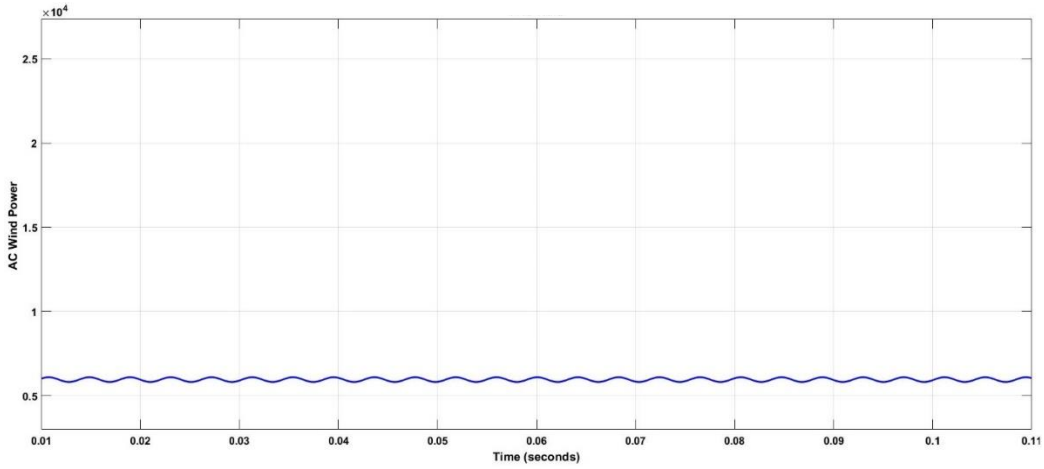

Fig. 4. 12.Wind turbine output power

The AC wind power output is an RMS power for the multiplication of RMS voltage and RMS current of the wind turbine.

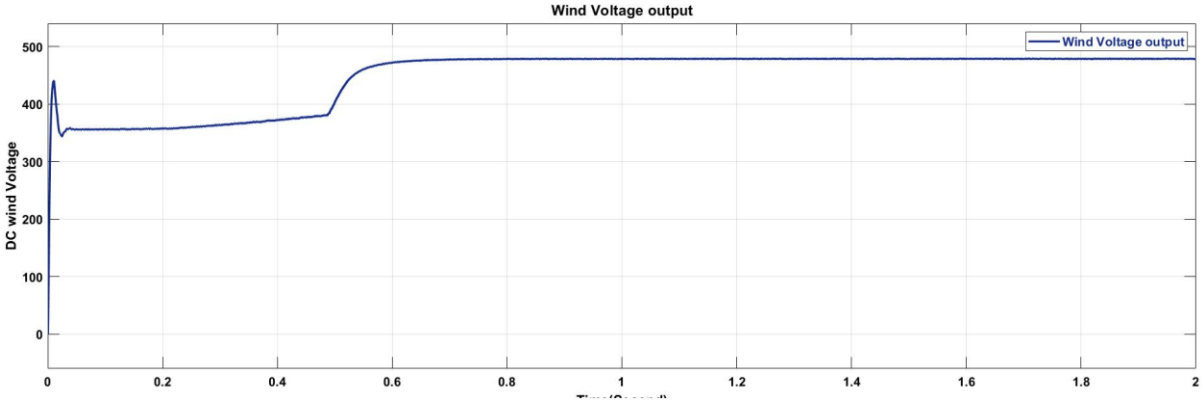

The battery stage of this project simulation is the third stage, and the results indicate the battery's state of charge (SOC), battery voltage, and battery current.

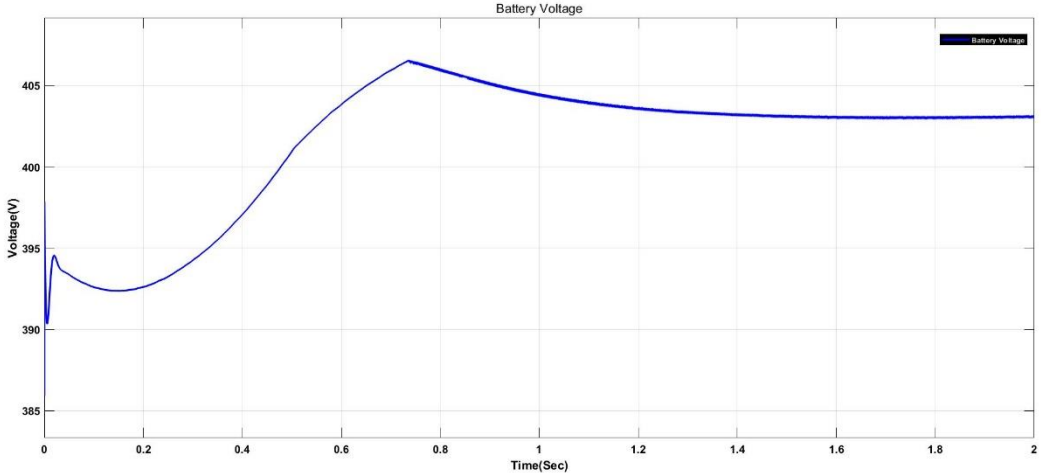

Fig. 4. 13. Battery output Voltage

The battery voltage is shown in Fig. 4.14; after the PV reaches MPPT, the battery voltage progressively increases until it reaches the maximum permitted value of 400 V, at which point it gradually decreases to stabilize the system.

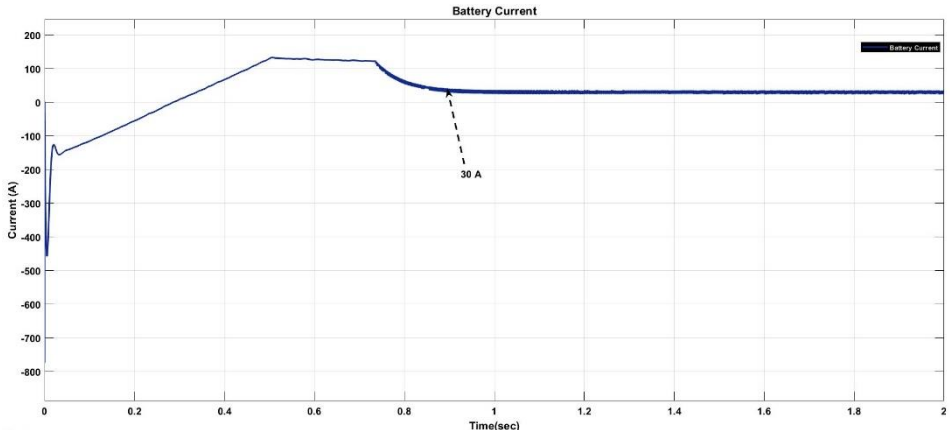

Fig. 4. 14. Battery output current

The battery current in Fig. 4.15 indicates that the battery voltage decreases first, and then the current rapidly increases until it reaches the reference current of 30 A. The charge and discharge states of the battery are depicted in Fig. 4.16.

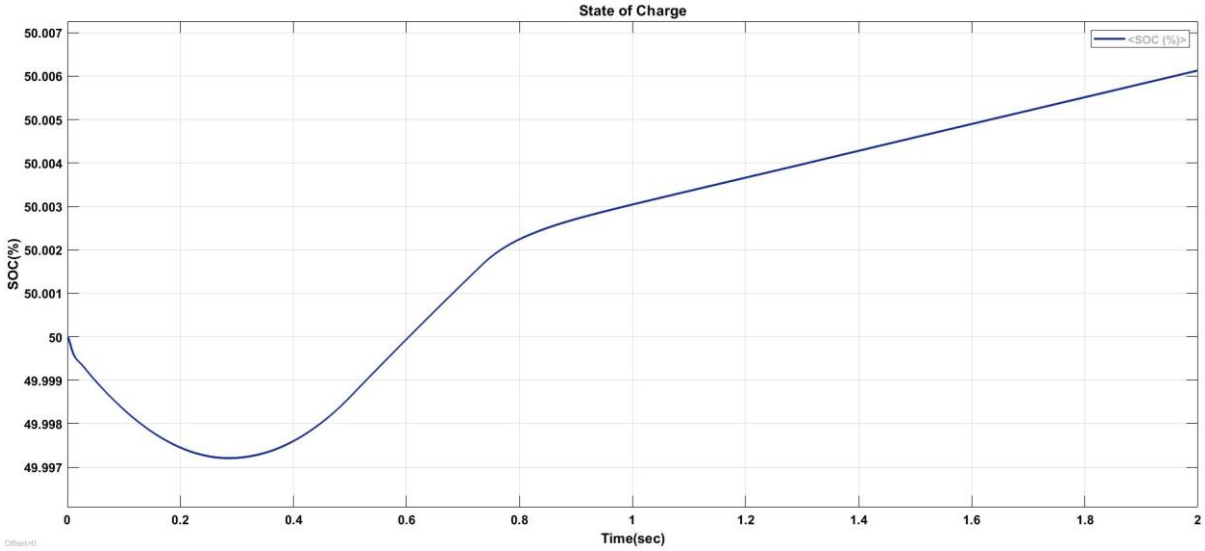

Fig. 4. 15. State of charge and discharge of the battery

When the time was zero, the status of charge was 50% because the PV was receiving low irradiation; when the DC link reached the rated voltage, the battery charged again. The system runs smoothly and is easy to use. The charging and discharging reference current is determined by the needed current load.

The DC link voltage is now shown in Fig. 4.17. The voltage remains constant until the time reaches 0.8 seconds. When the PV system approaches the MPPT, the voltage rises slightly and hits 417 V, which is the voltage point in an MPPT.

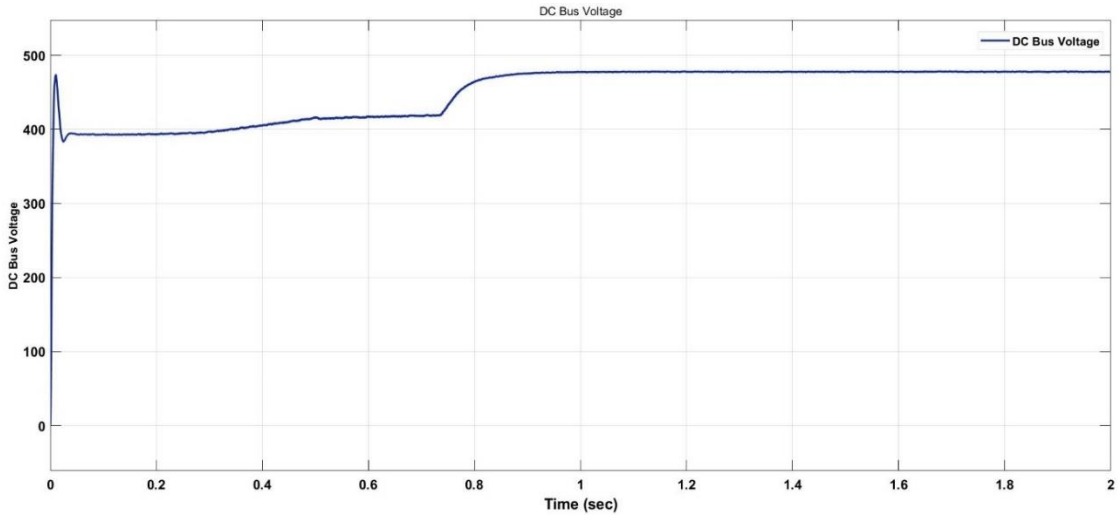

Fig. 4. 16. DC bus output voltage

The inverter is supplied with the DC link voltage, followed by an RLC filter to remove harmonics. The AC load is then connected, and the output voltage and current are displayed in Fig. 4.18. Phase to phase voltage is 400 V, while single-phase voltage is approximately 230V. The output current is proportional to the load connected. The system may be capable of

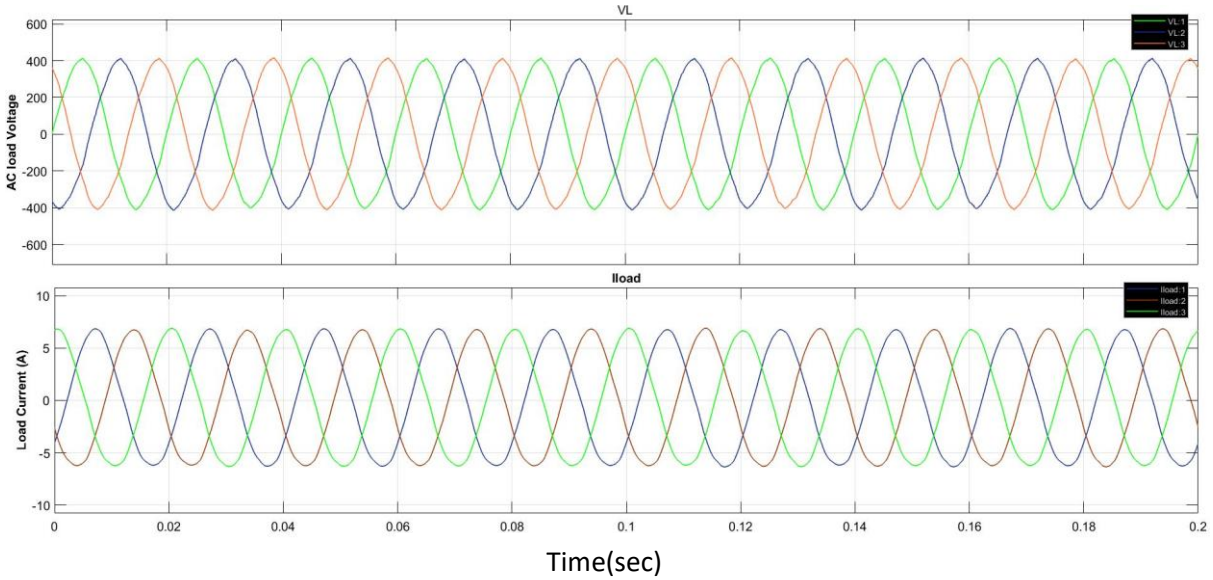

Fig. 4. 17. Load voltage and current

changing its load. The voltage and current are in phase, indicating that the system is providing load active power. The load power is depicted in Fig. 4.19.

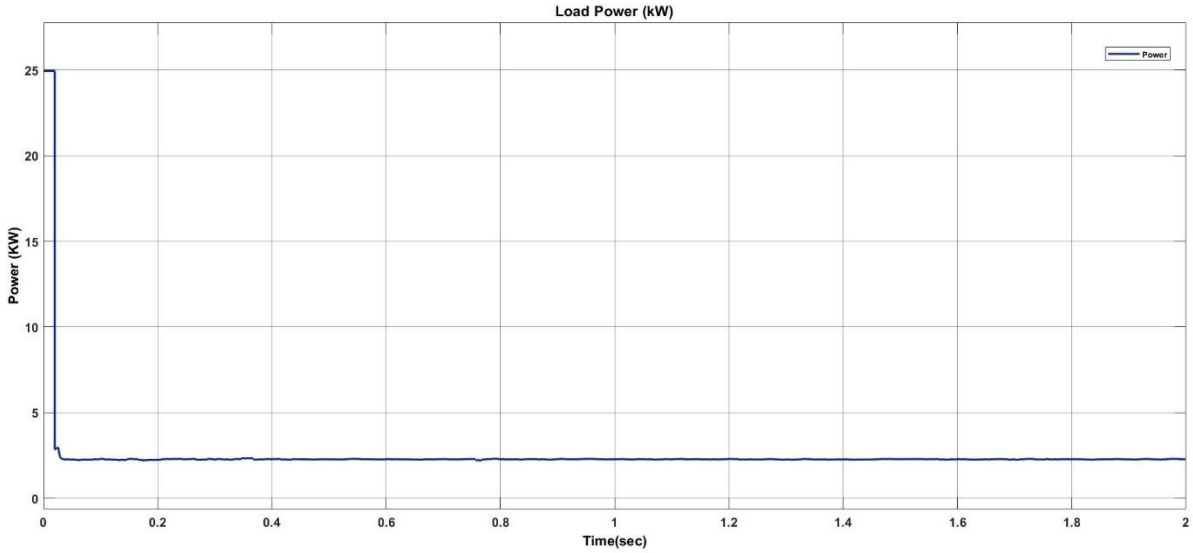

Fig. 4. 18. Load power (kW).

CHAPTER 5

Conclusion

The design of a cost effective hybrid standalone renewable energy system was examined in this study. A permanent magnet synchronous generator, photovoltaic system with MPPT algorithm, and Lead-acid Battery driven bidirectional charge controller, power electronic rectifier, and inverter are built to power the small wind turbine.

The renewable energy of the chosen place is represented by many sources. The data is then evaluated using a variety of data analysis methods. The analysed data is fed into the software, which then analyses the results. Additionally, the energy control and load supply continuity are met.

Various photovoltaic and battery sizing methods are studied during this study, and the optimum sizing computation is employed to build the perfect system sizing.

5.1 Future Work

The objective of this project is to determine whether hybrid renewable energy power is cost-effective in the selected location so that future research can focus on the following issues: power quality control, improved battery life cycle strategy, and mathematical modeling of the entire system. Because the existing Matlab/Simulink model of photovoltaic and wind turbines occasionally encounters stability issues, future researchers can implement the mathematical mode to avoid those issues.

5.2 Limitations

This project's limitations are summarized in the following statement.

1. The study focuses on determining the feasibility of a hybrid standalone renewable energy system using Homer Pro software.
2. One of the key limitations of this project is the lack of data availability, as no existing research or documents applying the data of the chosen location.
3. The system is designed using Matlab/Simulink.
4. Time constraints have also hampered the project's research and implementation.

Reference

[1] Edgar Ariel Escala Calame, “Local and Central Controllers for Microgrids,” M.S in Electrical Engineering (MSEE), University of Arkansas, Fayetteville, 2019.

[2] Erin Grisby *et al.*, “The Results of COP26,” Nov. 29, 2021. https://www.huntonnickelreportblog.com/2021/11/the-results-of-cop26/ (accessed Mar. 02, 2022).

[3] Jami Nelson Nuñez, “Powering Progress: The Potential of Renewable Energy in Somalia,” Somalia, Feb. 2015.

[4] World Bank, “Access to electricity (% of population) - Somalia | Data,” 2019. https://data.worldbank.org/indicator/EG.ELC.ACCS.ZS?locations=SO (accessed Mar. 02, 2022).

[5] epa.gov, “Distributed Generation of Electricity and its Environmental Impacts | US EPA,” *https://www.epa.gov/energy/distributed-generation-electricity-and-its-environmental-impacts*, 2020. https://www.epa.gov/energy/distributed-generation-electricity-and-its-environmental-impacts (accessed Mar. 02, 2022).

[6] M. F. N. A. T. K. and I. K. A. Ahmed, “An Overview on Optimal Planning of Distributed Generation in Distribution System and Key Issues,” in *IEEE Texas Power and Energy Conference (TPEC)*, 2021, pp. 1–6.

[7] Paulos Geremew Feyisa, “Energy Management System and Control of Standalone Photovoltaic System: (Case Study Ambo University Information Center Technology Building),” Thesis on M.Sc in Electrical Power and Control Engineering (Power Engineering), Adama Science and Technology University, Adama, Ethiopia, 2021.

[8] S. G. K. and M. R. S. Monesha, “Microgrid energy management and control: Technical review,” in *IEEE International Conference on Automatica (ICA-ACCA)*, 2016, pp. 1–7.

[9] Bradley Baxter, “Control of a Microgrid in Islanded and Grid-Connected Modes,” Thesis, Murdoch University, Perth, 2018.

[10] ANILA KUMARAN VADAKKEPURAKKEL MTECH-ENERGY SYSTEMS, “DESIGN of a HYBRID POWER GENERATION SYSTEM USING SOLAR-WIND ENERGY,” Deakin University, 2018.

[11] Tomas markvart, *Solar Electricity* , 4th ed., vol. 1. 2001.

[12] SANDEEP KUMAR, “MODELING AND SIMULATION OF HYBRID WIND/PHOTOVOLTAIC STAND-ALONE GENERATION SYSTEM,” Master of Technology in Industrial Electronics, National Institute Technology, Rourkela, 2017.

[13] D.P. Kothari, K.C. Singal, and Rakesh Ranjan, *Renewable Energy Sources and Emerging Technologies*, 2nd ed., vol. 1. New Delhi: PHI Learning Private Limited , 2011.

[14] solarmagazine, “Types of Solar Panels: On the Market and in the Lab [2020],” *solarmagazine*, 2020. https://solarmagazine.com/solar-panels/ (accessed Apr. 02, 2022).

[15] University of Central florida, “Cells, Modules, Panels and Arrays - FSEC Energy Research Center,” *FSEC Energy Research Center* . https://energyresearch.ucf.edu/consumer/solar-

technologies/solar-electricity-basics/cells-modules-panels-and-arrays/ (accessed Apr. 02, 2022).

[16] Prof. Shireesh B. Kedare, “Wind Energy Conversion Systems ,” *ENERGY SYSTEMS ENGINEERING INDIAN INSTITUTE OF TECHNOLOGY, BOMBAY* , BOMBAY , pp. 1–20, 2016.

[17] Shahidul I. Khan, Mohammad Upal Mahfuz, Tareq Aziz, and N. M. Zobair, “Prospect of Hybrid Wind System in Bangladesh,” 2002.

[18] Dan Chiras, *Power from the Wind: Achieving Energy Independence A Practical Guide to Small-Scale Energy Production*, 2nd ed., vol. 1. New Society Publishers, 2017.

[19] Jean-Claude Sabonnadière, *Renewable Energy*, 1st ed., vol. 1. 2009.

[20] Chia-Nan Wang, Wen-Chang Lin, and Xuan-Khoa Le, “Modelling of a PMSG Wind Turbine with Autonomous Control,” *Hindawi*, vol. Volume 2014, no. 27 May 2014, 2014.

[21] Francisco Gonçalves Goiana Mesquita, “Design Optimization of Stand-Alone Hybrid Energy Systems,” FACULDADE DE ENGENHARIA DA UNIVERSIDADE, DO PORTO, 2010.

[22] A. Doolittle Georgia Tech, “ECE 4833-Dr.”

[23] Farzam Nejabatkhah, Yun Wei Li, Alexandre B. Nassif, and Taeho Kang, “Optimal Design and Operation of a Remote Hybrid Microgrid,” *CPSS TRANSACTIONS ON POWER ELECTRONICS AND APPLICATIONS*, vol. VOL. 3, pp. 1–20, 2018.

[24] Chowdhury Akram Hussain, Nusrad Chowdhury, Michelo longo, and Wahiba Yaici, “System and Cost analysis of standalone solar home system applied developing country,” *sustainability* , vol. 11, 2019.

[25] A. Dolara, E. Donadoni, S. Leva, G. Magistrati, and G. Marchegiani, “Performance analysis of a hybrid micro-grid in Somalia,” Jul. 2017. doi: 10.1109/PTC.2017.7980867.

[26] Chowdhury Akram Hussain, Nusrad Chowdhury, Michelo longo, and Wahiba Yaici, “System and Cost analysis of standalone solar home system applied developing country,” *sustainability* , vol. 11, 2019.

[27] Waqas Ali, Haroon Farooq, and Ata Ur Rehman, “Design Considerations of Stand-Alone Solar Photovoltaic Systems,” *IEEE*, vol. 12, 2018.

[28] Shahriar A. Chowdhury, S. M. Raiyan Kabir, and S. M. Moududuł Islam, “Technical Appraisal of Solar Home System Equipments in Bangladesh,” *Researchgate*, 2019.

[29] Omar Assowe Dabar, Mohamed Osman Awaleh, Daniel Kirk-Davidoff, Jon Olauson, Lennart Söder, and Said Ismael Awaleh, “Wind resource assessment and economic analysis for electricity generation in three locations of the Republic of Djibouti,” *sciencedirect*, 2019.

[30] G. S. Dusmareb, “Global Solar Atlas,” 2022. https://globalsolaratlas.info/map?s=5.536077,46.383084&m=site&c=5.536077,46.383084,11 (accessed Mar. 16, 2022).

[31] “Sizing PWM Solar Charge Controllers - DIY Solar Resources.” https://www.altestore.com/diy-solar-resources/sizing-pwm-solar-charge-controllers/ (accessed Mar. 18, 2022).

[32] “Hybrid SMA inverter SMA Tripower 10.0 | Alma Solar® Nr. 1 of online solar panels.” https://www.alma-solarshop.com/sma-inverter/1460-hybrid-sma-inverter-sma-tripower-100.html (accessed Mar. 18, 2022).

[33] Solomon Teklemichael Bahta, “Design and Analyzing of an Off-Grid Hybrid Renewable Energy System to Supply Electricity for Rural Areas (Case Study: Atsbi District, North Ethiopia),” Master of Science Thesis, KTH Industrial Engineering and Management, Stockholm, Sweden, 2013.

[34] Ahammad, “DESIGN STRATEGY FOR AN OFF-GRID SOLAR-WIND HYBRID POWER SYSTEM,” MASTER OF SCIENCE IN ELECTRICAL AND ELECTRINIC ENGINEERING, BANGLADESH UNIVERSITY OF ENGINEERING AND TECHNOLOGY, DHAKA, BANGLADESH, 2014.

[35] “How Much Does Wind Turbine Cost In 2022?” https://costaide.com/wind-turbine-cost/ (accessed Mar. 27, 2022).

[36] Musadag El Zein, “OFF-GRID WIND POWER SYSTEMS: PLANNING AND DECISION MAKING,” Thesis, Uppsala University, Campus Gotland, 2019.

[37] Tomas markvart, *Solar Electricity* . 2001.

[38] A. Kumaran Vadakkepurakkel, “DESIGN of a HYBRID POWER GENERATION SYSTEM USING SOLAR-WIND ENERGY,” 2018.

[39] T. H. M. S. Rashid, A. K. Routh, R. Rana, A. H. M. I. Ferdous, and R. Sayed, “A Novel Approach to Maximize Performance and Reliability of PMSG Based Wind Turbine: Bangladesh Perspective,” *American Journal of Engineering Research (AJER*, no. 7, pp. 17–26, 2018, [Online]. Available: www.ajer.org

[40] C. N. Wang, W. C. Lin, and X. K. Le, “Modelling of a PMSG wind turbine with autonomous control,” *Mathematical Problems in Engineering*, vol. 2014, 2014, doi: 10.1155/2014/856173.

[41] S. Kumar, “MODELING AND SIMULATION OF HYBRID WIND/PHOTOVOLTAIC STAND-ALONE GENERATION SYSTEM A THESIS SUBMITTED IN PARTIAL FULFILLMENT OF THE REQUIREMENTS FOR THE AWARD OF THE DEGREE OF Master of Technology in Industrial Electronics Department of Electrical Engineering.”

Appendix

A.1. Matlab Code for Parameter Calculation

```
%% Solar PV Array Sizing and Specifications
% Choosen one Jinko Solar
P= 400.32; %watt
Vpm = 41.7; %V
Ipm = 9.6; %A
Ppeak = 200e3; %W
Vsystem = 400;
Isystem = Ppeak/Vsystem;
Nmp = round(Isystem/Ipm);%number of modules paralel
Nms = round(Vsystem/Vpm);%number of modules series
Tm = Nms*Nmp; % Total Pv Modules
CP_Watt = 0.5; %cost of per watt in USD
CM = CP_Watt*P; % cost per module in usd
TC = CM*Tm;% Total Cost of PV Panels
kWcost = TC/Ppeak*1000; % 1kW cost
MTWICost = 980; % Mounting, Tracking,Wiring and Installation
Cost
CostkW = kWcost+MTWICost; %total cost per kW
%% Battary Sizing and specifications
%choosen one Lead Acid Battery
Vnominal = 12; %v
BaC = 260; % selected capacity Watt hour
DOD = 0.85;% dept of discharge
DA = 2; %days of autonomy
Oeff= 0.8; %ouput efficiency
AP = 200; %average power kW
ED =AP*24; % Energy Demand Per day
BC= round((ED*DA)/(DOD*Oeff));% Battery Capacity Ah
Bp = round(BC/BaC); %Parallel Batteries
Bs= round(Vsystem/Vnominal)-1; % Series batteries
TB = Bp*Bs; % total number of batteries
BCost = 140; %usd one piece
CIcost = 270; %Charge controller and installation cost
TBC_1P = BCost+CIcost; %total one Battery cost
TCOB = TBC_1P*TB; % Total Cost of Bataries
%% Wind Turbine Sizing and Specifications

%% Boost Converter
Vinput = 390;
Vou = 400;
Prated = 200e3;
Fs = 5e3;
Current_ripple = 5;%
Voltage_ripple = 1;%
Input_current = Prated / Vinput;
Current_rippl = 0.05*Input_current;
Voltage_rippl = 0.01*Vou;
```

```
Output_current = Prated/Vou;
Inductance = (Vinput*(Vou-Vinput))/(Fs*Current_rippl*Vou);
Capacitance = (Output_current*(Vou-
Vinput))/(Fs*Voltage_rippl*Vou);
%% Calculation of Buck Converter
%specification
Pr = 200e3;
Vin = 400;
Vout = 360;
RC = 0.05; % 5% Ripple Current
RV = 0.01; % 1% Ripple Voltage
sf = 5e3; %switching Frequency
Io = Pr/Vout; %output Current
CR = RC*Io; %Current Ripple
VR = RV*Vout; %Voltage Ripple
L = (Vout*(Vin-Vout))/(sf*CR*Vin); % inductor Value
C = (CR)/(8*VR*sf); % capacitor current
```

A.2. System Cost Summary from HOMER Pro

Component	Capital ($)	Replacement ($)	O&M ($)	Fuel ($)	Salvage ($)	Total ($)
Discover 12VRE-3000TF	$641,240.00	$230,529.73	$202,186.36	$0.00	-$92,659.94	$981,296.14
Generic 10 kW	$150,000.00	$0.00	$38,782.55	$0.00	$0.00	$188,782.55
Generic flat plate PV	$1,512,073.82	$0.00	$0.00	$0.00	$0.00	$1,512,073.82
System Converter	$34,518.98	$0.00	$0.00	$0.00	$0.00	$34,518.98
System	$2,337,832.80	$230,529.73	$240,968.91	$0.00	-$92,659.94	$2,716,671.49

A.3. Drive Drain and Pitch Control Model of Wind Turbine